Petahertz Electronics

Christian Heide,[1,2,*] Phillip D. Keathley,[3] and Matthias F Kling[1,2]

[1]*Department of Applied Physics, Stanford University, Stanford, CA 94305, USA*

[2]*Stanford PULSE Institute, SLAC National Accelerator Laboratory, Menlo Park, CA 94025, USA*

[3]*Research Laboratory of Electronics, Massachusetts Institute of Technology, 77 Massachusetts Ave, Cambridge, 02139, MA, USA*

(Dated: May 31, 2025)

* cheide@stanford.edu

Despite tremendous efforts of the semiconductor industry, the clock rate of today's electronics has leveled off to a few gigahertz. Effects associated with using pulsed voltages prevent the scaling of clock rates beyond the gigahertz level. To break through this gigahertz barrier, alternative methods for controlling the flow of charge carriers are being sought. Petahertz electronics, also known as lightwave electronics, introduces a new concept: Instead of pulsed voltages, it uses tailored optical waveforms to control charge carriers in an electronic circuit at petahertz frequencies. A sizeable body of research has demonstrated such petahertz-sale currents driven by optical fields within and around solid-state systems and nanoscale structures. The analog age of petahertz electronics is underway, with several proof-of-principle demonstrations of sub-optical-cycle current generation and optical-field-resolved waveform detection at the sub- to few-femtosecond scale. Recent work has taken the first steps toward digital and quantum operation by demonstrating optical-field-driven logic and memory functionality. Here, we review the progress toward petahertz electronics, highlighting key theoretical concepts, experimental milestones, and questions remaining as we push toward realizing digital petahertz electronics for potential ultrafast optical waveform analysis, communications, and quantum computation.

I. INTRODUCTION: PETAHERTZ ELECTRONICS

The development of electronic devices has been the basis for the unprecedented technological progress of the twentieth century. Early on, it was realized that electromagnetic radiation could transfer information through air and materials at high speeds [1]. To harness this capability, rectifying elements such as vacuum tubes were developed to convert the information stored within these oscillating electromagnetic waves to and from electrical currents for transmission and readout. With devices that could rectify electromagnetic fields came the use of radio waves for critical applications such as communication and ranging. All-electronic switches such as vacuum tube triodes and transistors were developed later to create logic gates for computing, heralding the age of microelectronics.

Due to the properties of the materials used for modern electronics, current injection and switching speeds are limited to the gigahertz to terahertz scale, as depicted in the bottom left

of Fig. 1. While the frequency of electromagnetic radiation can be continuously increased, a limit is reached at which the photon energy is sufficient to inject charge across energy barriers, and the field is no longer the primary driver of current. **In this regime, charge injection follows the square of the cycle-averaged envelope of the light's electric field waveform, meaning that octaves of bandwidth, resulting in single-femtosecond lase pulses are required to achieve a petahertz-fast electronic responses. While waveform synthesis might achieve such bandwidths [2], this approach is not easily scalable.**

To overcome this bandwidth constraint, nonlinearities can of course be leveraged. At ~~these~~ optical frequencies (on the petahertz scale, i.e., approaching and exceeding 100s THz), field-level interactions such as nonlinear wave mixing and optical switching **that** leverage nonlinear optical materials such as crystals [3] **can be used to excite charge carriers**. **However,** ~~F~~for efficient nonlinear interaction in these materials, extended interaction regions are required for phase-matching, **and a separate optical detection medium is required for conversion to an electronic response,** limiting the compact realizations of optical on-chip devices for applications such as computing.

To relax constraints on excitation bandwidth within a compact form-factor, ~~A~~**a**lternative materials and systems that continue to behave electronically when driven at optical frequencies have been sought. That is, devices and systems where the emitted current has a non-perturbative electronic response, directly sensitive to the field of the driving light waveforms rather than their time-averaged intensity. **These systems are the main focus of this review.**

The first experiments utilizing a light wave to control the flow of electrons were demonstrated in the gas phase, where a strong optical field tunnel ionizes an atom within a fraction of an optical cycle. The optical field of light then accelerates the freed electron and drives it subsequently back to its parent ion, releasing its excess energy through a burst of high-frequency radiation, a process called high-harmonic generation (HHG), which heralded the birth of attosecond science [4–6]. Combined with stabilized frequency combs, it became possible to trigger and steer the microscopic motion of electrons in a vacuum with precision limited only by quantum mechanical uncertainty [7].

Soon afterward, it was realized that such petahertz-scale electron control is also possible from the surface of nanoparticles [8] and nanoscale needle tips [9, 10]. Compared to atoms,

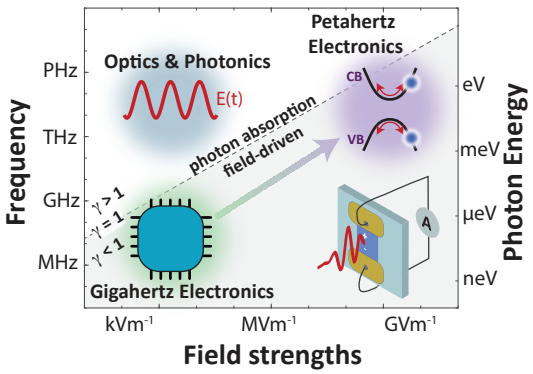

FIG. 1. **Electric-Field vs. Photon-Driven Electronics.** In today's gigahertz electronics, electric fields with a strength of around $E_0 \sim 0.1$ kV/m control the current flow, allowing for switching, rectification, and, ultimately, computing. In optics, the electromagnetic fields oscillating at 100 terahertz to petahertz frequencies can be generated using laser sources. However, with increasing frequency, a limit is reached where the charge generation mechanism inside of solids is slow compared to the cycle duration of the driving field, and cycle-averaged photon-based absorption governs the device response. **In this regime octaves of spectral bandwidth are needed at optical frequencies in order to generate petahertz-scale carge carriers.** ~~To increase the speed of current generation in the solid~~ **An alternative approach to increase the speed of current generation in the solid lies in the use of field-driven currents.** ~~particularly at~~**At** petahertz**-scale** frequencies, an electric field strength of $E_0 \sim$ GV/m is required **to achieve sub-cycle, field-driven current injection in typical solids** (see Box 1 **for further discussion**). These fields can be achieved with tailored ultrashort laser pulses. The gray-dotted line represents the condition where the driving frequency equals the frequency of current injection in GaAs, i.e., $\gamma = 1$ (see Box 1 for detailed discussion around **the Keldysh parmater** γ). Below this line, the current generation mechanism is sensitive to the electric field waveform, whereas above, the response is governed by photon absorption. The scale on the right indicates the associated photon energy.

a particular advantage of nanostructured optical-field emitters is their compactness and the enhanced electric field at the structure's apex, caused by the dynamic lightning rod effect that enables broadband field enhancement of around 35, depending on the material, shape, and wavelengths used [11, 12], relaxing the need for bulky, high-intensity laser systems. This has since been extended from needle tips to planarized nanostructures on chip surfaces [13–15]. Sub-cycle electron emission at hundreds of THz to PHz has since been demonstrated in nanoantenna arrays, with optical fields driving the tunneling emission of electrons [16–22].

Electron control inside solids was initially considered unsuitable for petahertz-fast current control. In particular, when the photon energy approaches the bandgap, the charge carrier becomes excited via resonant absorption, which is not primarily field-driven and results in thermal heating and, eventually, damage to the solid. Furthermore, scattering processes

and hence low coherence times, carrier screening, and a low damage threshold were deemed unsuitable. However, with the observation of non-perturbative high-harmonic generation and sub-femtosecond solid-state spectroscopy, it turned out that light-field-driven electron dynamics inside solids at petahertz frequencies is possible [23–31].

The first demonstration of light-field-induced current control in fused silica, a dielectric material [26], dates about a decade ago. Since then, various compact, chip-scale elements have demonstrated the control of charge carriers at petahertz frequencies and the creation of sub-femtosecond current bursts in a range of materials and systems, including the semimetal graphene [30, 32–35], semiconductors [36–38], and dielectrics [26, 38–40]. In analogy with tera- and gigahertz electronics, this platform has been coined *petahertz electronics* [16, 17, 41, 42]. Compared to the first experiments in dielectrics, the required peak energy has been reduced by ten orders of magnitude through the application of novel materials and miniaturization, nanoplasmonics, pump-probe schemes, and the development of powerful waveform-controlled high repetition-rate light sources in the near- and mid-infrared spectral range, making this technology accessible to many laboratories and applications.

While some challenges and open questions remain, which we will elaborate on later, petahertz electronic components and future signal processing are now clearly within reach. Recently, a logic gate [43], light-field current switching [26, 44], random-access memory (RAM) [45], spin- and valleytronics [46–50], Bloch electron wave control and splitting at ambient temperature [30, 35], and data encoding [51, 52] have been predicted and demonstrated at terahertz to petahertz frequencies. In addition, petahertz-scale light-field sampling has been pioneered [18, 26, 53–56], analogous to a sampling oscilloscope for optical field waveforms, providing critical tools for fundamental science and the further analysis and development of petahertz electronics.

Beyond the technological progress of petahertz electronics, coherent lightwave control of charge carriers in solids has recently found tremendous interest in material spectroscopy, as it provides direct access to novel solid-state properties, such as quantum-mechanical phases [25, 35], topological properties [57–60], strong electron correlations [61–63], and ultrafast magnetism [64], offering a new paradigm for future lightwave spectroscopy and electronics [65].

In this article, we will start by reviewing the fundamentals of petahertz electronics, which are the sub-cycle electric field response in condensed media (II B 1), at interfaces (II B 2), and

at nanostructured systems (II B 3). Afterward, we review applications that have ushered in the analog age of petahertz electronics, with carrier-envelope phase detection (III 1) and sub-cycle optical field sampling (III 2). Finally, we review theoretical proposals for transitioning from analog petahertz electronics to integrated classical and quantum-based petahertz logic operations (IV).

II. FUNDAMENTALS

A. Sub-Cycle Electric Field Response

Petahertz electronics, as we refer to it here, refers to the condition where optical-field-sensitive currents having petahertz-scale frequency content are both generated and subsequently detected. We will begin by briefly reviewing the criteria to generate a petahertz-fast (sub-femtosecond) current response inside a solid.

When a lightwave interacts with electrons in the band structure, the optical field of light $E(t)$ transiently accelerates Bloch electrons by imparting a **time-dependent** momentum $\dot{k}(t)$ to the electrons. The amount of momentum transferred is described by Bloch's acceleration theorem [66]

$$\dot{k}(t) = e\hbar^{-1}E(t), \tag{1}$$

with e the elementary charge and $\hbar$ the reduced Planck constant. Equation (1) is valid independent of the applied field strengths and frequency and generates an oscillating dipole. This does, however, not mean that a measurable current sensitive to the exact shape of $E(t)$ emerges. To obtain a residual current sensitive to the shape of $E(t)$, which can be measured within a circuit, it needs to be generated and retained in the system within a time scale below the cycle duration of the driving optical waveform. In the context of the current generation within a solid, the crucial parameter describing the speed of the current generation is the time it takes for an electron to undergo a band-to-band transition [67–69]. Likewise, at a material interface, such as a metal-vacuum or material-material transition, the tunneling time sets the speed limit. The associated frequency is defined as angular tunnel frequency ω_t. Both cases are discussed and illustrated in Box 1. This condition also refers to the *strong-field* or *light-field driven* regime, originally categorized by the Keldysh

adiabaticity parameter $\gamma = \omega/\omega_t$ [67, 69, 70], **with ω the angular frequency of the oscillating lightwave**. In Box 1, we compare the electron dynamics upon laser excitation of the two systems: **(a)**~~(1)~~ at a solid with valence and conduction band states and **(b)**~~(2)~~ at a metal surface with tunnel ionization. If $\gamma < 0$, the electrons transition from one to the other band or from the metal to vacuum (Box 1) occurs on a sub-cycle timescale (see right panels in Box 1 **a**, **b**) and thus the excitation or ionization is sensitive to $E(t)$. For $\gamma > 0$, the transition time is too slow to generate a residual current sensitive to the electric field waveform, and the electron dynamics follow the time-averaged intensity of the excitation pulse and thus do not respond to optical frequencies.

To speed up the transition frequency and ultimately obtain a system response sensitive to $E(t)$, the electric field amplitude that drives the current needs to be increased, also illustrated as the gray dashed line in Fig. 1. Both regimes are discussed in further detail in Box 1, and typical field-strengths values for petahertz electronics of ∼V/nm are derived.

One possibility to increase the peak electric field strengths of the laser pulse without damaging the material is to decrease the pulse duration while maintaining the pulse energy. Combined with ~~plasmonic~~**tight focusing, resonant systems, such as plasmonics, in addition to** nanostructure**d features for geometric field enhancement**~~s and tight focusing~~, it is possible to obtain field strengths in the order of ∼V/nm from picojoule laser pulses. Furthermore, with frequency combs [71], it became possible to stabilize and synthesize optical lightwaves, similar to what was done for radiowaves, which was an essential breakthrough in precisely controlling electrons in free space or solids [7, 13, 14, 16, 17, 30, 33, 34, 36–39, 43, 71–74].

Box 1: Required Optical Field Strengths for Sub-Cycle Current Generation.

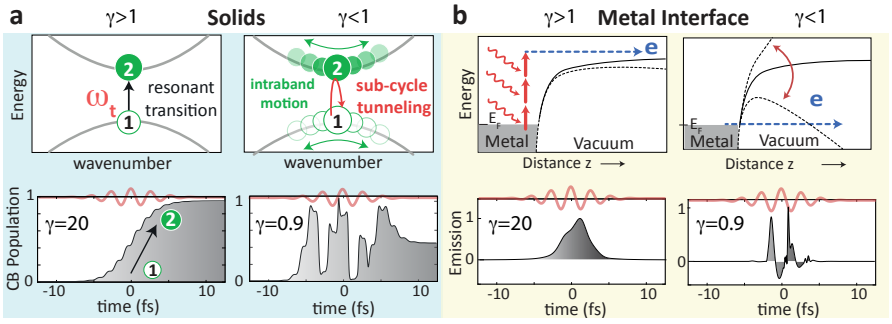

Electron Dynamics in Condensed Media and at Metal Interfaces. a,

Schematic illustration of the electron dynamics in the conduction and valence band (top panel) and time-resolved population dynamics (bottom panel). For $\gamma = 20$, the population builds up gradually during the laser pulse. The additional oscillation, which is twice the frequency of the laser, is known as Bloch-Siegert oscillation. For $\gamma = 0.9$, the electron dynamics is faster than an optical cycle of the driving pulse. ***b****, Light-induced tunnel ionization from a metal surface (top panel) and corresponding temporal emission (bottom panel, $\gamma = 20$ and $\gamma = 0.9$).*

In electronics, when the frequency of the electromagnetic field increases, a limit is reached where ω becomes higher than ω_t, and the field is no longer the primary driver of current. To speed up the tunneling frequency, the electric field strengths need to be increased. Here, we estimate typical values for the electric field to be sensitive to the petahertz control in condensed media and at metal surfaces.

- **Sub-Cycle Band-to-Band Transition in GaAs (Condensed Media, Bound-to-Bound Transition), Figure a** The tunneling frequency from a band-to-band transition can be estimated as $\omega_t = \frac{\sqrt{m_{\mathrm{e,\,eff}}\Delta}}{eE_0}$. To obtain $\gamma < 1$ in GaAs (**effective electron mass:** $m_{\mathrm{e,\,eff}} = 0.067m_e$, **band gap:** $\Delta = 1.42$ eV, **electron mass:**m_e the electron mass) at 0.375 PHz (**central wavelength** 800 nm) and, a minimal electric field strength of $E_0 = 1.7\,\mathrm{V/nm}$ is required. Here, we note that the Keldysh parameter can also be approximated and understood in terms of the ratio of the driving frequency and the half a Rabi cycle $\Omega_R = \frac{dE(t)}{\hbar}$, i.e., $\gamma \sim \frac{\omega}{2\Omega_R}$, with d the transition dipole moment. For GaAs with $d = 0.5\,e\,\mathrm{nm}$, we obtain $1.5\,\mathrm{V/nm}$ as the minimal field strengths to drive a band-to-band transition on a sub-cycle timescale. This regime is also known as carrier-wave Rabi flopping. Figure **a** shows the temporal evolution of the conduction band for $\gamma > 1$, (left panel) and $\gamma < 1$ (right panel).
- **Sub-Cycle Tunnel Ionization (Metal Interface, Bound-Continuum Transition), Fig. b** In the case of tunnel ionization from metal to vacuum, the tunnel frequency can be estimated as $\omega_t = \frac{eE_0}{\sqrt{2m_e\Phi}}$, with Φ the work function of the metal. The work function of typical metals is on the order of $\Phi = 5$ eV. To estimate the required field to obtain a sub-cycle response, i.e., $\gamma < 1$, at 0.375 PHz, a field strength of at least 18 V/nm is required to drive sub-cycle tunnel ionization. Figure **b** (bottom panel) shows the temporal emission profile. For $\gamma < 1$, the emission follows the intensity envelope of the laser pulse, whereas for $\gamma > 1$, the emission dynamics are sensitive to the electric field waveform.

Based on the Keldysh approximation, we can see that **(i)**~~(1)~~ to build petahertz electronics using semiconductors with a band gap of ∼eV, an electric field strength on the order of ∼V/nm is required, and **(ii)**~~(2)~~ in the case of sub-cycle tunnel ionization from a metal surface, a ten-times higher electric field strength is required compared to sub-cycle band-to-band transition in semiconductors. The lower electric field strengths in semiconductors compared to metals (or atoms) can be understood based on the reduced energy gap to transition from one state to another. The bandgap is typically smaller than the ionization potential in metals and secondly, the effective electron mass is smaller in semiconductors, compared to free space ($m_{\mathrm{e,eff}} < m_{\mathrm{e}}$).

B. Systems and Materials for Petahertz Electronics

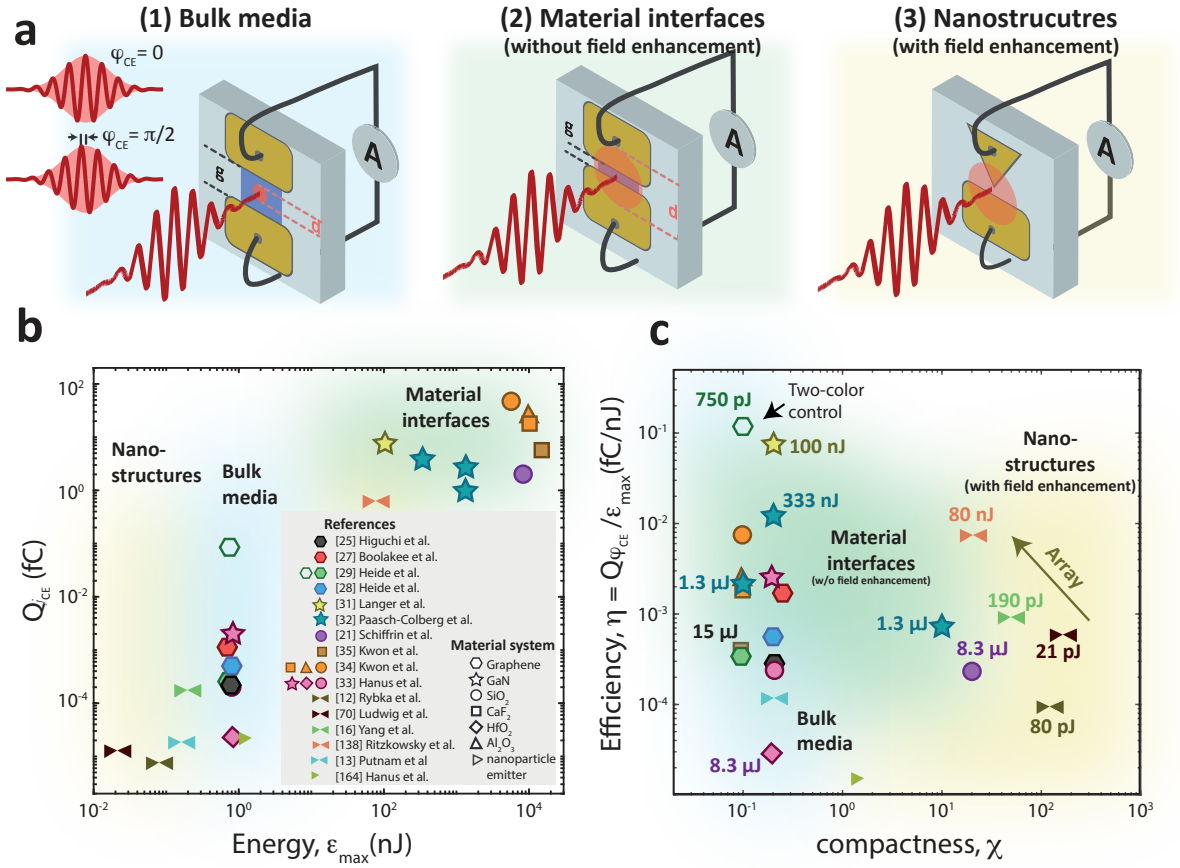

FIG. 2. **Recent Progress in Petahertz Current Injection. a,** Device schemes for current injection in (1) bulk media (spot size smaller than g), (2) at material interfaces (spot size smaller than g), and (3) at nanostructured systems with optimized field enhancement. **b,** Maximal CE phase -sensitive charge injection $Q_{\varphi,\mathrm{CE}}$ plotted as a function of pulse energy for various material systems (semimetal: graphene [30, 32–34], semiconductor: GaN[36–38], dielectrics: SiO_2[26, 38, 39], CaF_2[39, 40], HfO_2[38], Al_2O_3[39], and nanogaps [13, 14, 17]. The three device schemes are highlighted in blue (bulk media), green (material interface, without field enhancement), and yellow (nanostructured systems designed for maximal field enhancement). **c,** To compare various experimental conditions, we plot the efficiency η, defined as the ratio of $Q_{\varphi,\mathrm{CE}}$ and pulse energy $\varepsilon_{\max}$, versus the device's compactness χ (inverse electrode separation g). More relevant experimental parameters and a performance comparison can be found in the Supplementary Information.

Figure 2 summarizes the experimental progress of petahertz-scale current generation inside of **(1) Bulk Media, (2) Material Interfaces and (3) Nanostructures** ~~condensed media (1), at material interfaces (2), and at nanostructured systems (3)~~. Throughout the discussion of the microscopic mechanisms of the current generation, Fig. 2 with its labels **(1)-(3)** will

serve as an outline.

To inject the petahertz-scale current, phase-stabilized few-cycle laser pulses are used, as illustrated in Fig. 2 **a**. The field oscillations' timing to the pulse peak is determined by the carrier-envelope phase φ_{CE}. For few-cycle laser pulses, a change in the CE phase substantially changes their temporal evolution. This is shown for a few-cycle long cosine or sine-like waveform in Fig. 2 **a**. By changing φ_{CE}, the degree of time asymmetry of the laser pulse can be controlled, which may result in a non-zero residual petahertz current.

Figure 2 **b** and **c** show a comparison of the experimentally demonstrated petahertz-fast current generation in various materials and systems, such as in the semimetal graphene [30, 32–34], semiconductors [36–38], dielectrics [26, 38–40], and on-chip nanogaps and nanogap arrays made from metallic needles [13, 14, 17, 18, 20, 75, 76]. For this, we plot the waveform-sensitive injected charge Q_{φ} versus the applied pulse energy $\varepsilon_{\mathrm{max}}$ in Fig. 2 **b**. Furthermore, we plot the efficiency, $\eta = Q_{\varphi}/\varepsilon_{\mathrm{max}}$ versus the device's compactness (inverse electrode distance) in Fig. 2 **c**. Compactness might become relevant in future miniaturized devices, where many components must be positioned in a finite area (or volume). Before comparing the efficiency and performance of these systems in detail, we first discuss the underlying current generation mechanisms for each case.

1. *Condensed Media*

We start our discussion with case (1) **Bulk Media**: A CEP-stabilized laser field illuminates the solid and injects a residual waveform-sensitive current measured with two metal electrodes. We note that such measurements have been performed via photon-based ($\gamma > 1$) quantum-path interference (known as quantum control) for more than 30 years using two- or multi-color fields [77–80], however, these currents are not generated on a sub-cycle timescale of the laser field; hence this scheme is not well suited for petahertz electronics**, see temporally resolved electron dynamics in Box 1**. Here, we focus on the strong-field counterpart with sub-cycle current injection, i.e., $\gamma < 1$ (see Box 1).

With CEP stable few-cycle laser pulses, it has been demonstrate that intraband motion and interband transitions are coupled at large field strengths, and that electrons undergo Landau-Zener transitions between valence and conduction band, and not only just once, but the electrons can undergo two subsequent Landau-Zener transitions when they are driven

back and forth across the apparent band gap minimum by the oscillating light field (Fig. 3 **a** and **b**) [30, 33, 44]. At **a wavelengths of** 800 nm these two transition events are only separated in time by half an optical cycle, so roughly 1.3 fs. Because of this short time, this happens fully coherently, so that electronic matter wave coherence is preserved. Since the Landau-Zener transition events act as electron beam splitters, with two subsequent transitions an electron interferometer akin to a Mach-Zehnder interferometer for light has been demonstrated. The quantum phase accumulated in the beam-split state determines in which output port the electron ends up: in the valence or the conduction band. This type of interferometer is called a Landau-Zener-Stückelberg-Majorona (LZSM) interferometer [81–84]. Intriguingly, the interferometer action happens so fast that for an asymmetric vector potential a current emerges within one femtosecond. **We note that the underlying mechanism is an complex interplay between the shape of the band structure, the dipoles and the strength and frequency of the laser field, ultimately defining the splitting ratio and the amount of accumulated phases. The effects described here are of a general nature and can in principle be observed in various solids. Here, we particularly focus our discussion on graphene as an ideal model system for such measurements, as it has a high conductivity, which facilitates current measurement and a simple band structure.** To experimentally demonstrate petahertz-fast current injection in graphene, few-cycle laser pulses are focused on the center of a symmetric electrode-graphene-electrode device.

~~Changing the asymmetry of the waveform by means of φ_{CE} or by adding a second color causes the resulting current in graphene to oscillate as a function of asymmetry (Fig. 3e). Furthermore,~~ By increasing E_0, the measured current scales non-monotonically, with several current reversals around 2 and 3 V/nm (Fig. 3 **e**) [33, 35], indicating, LZSM interferometry. The observation of LZSM interferometry in graphene highlights **(i)**~~(1)~~ the field of light controls electrons at optical frequencies, **(ii)**~~(2)~~ LZ transitions are occurring on petahertz frequencies, i.e., on a sub-cycle timescale of the driving field, **(iii)**~~(3)~~ the electron dynamics during an optical cycle is coherent, and **(iv)**~~(4)~~ based on a comparison with model simulations, the residual current peaks for $\varphi_{\mathrm{CE}} = \pm\pi/2$, i..e, when $A(t)$ breaks the inversion symmetry. Similarly to graphene, a non-perturbative current increase has also been found in GaN, HfO_2, and SiO_2 (Fig. 3 **f**) [26, 36–40]. **However, in these measurements, a non-monotonic current response as a function of E_0 has not been observed, most**

likely because compared to graphene, these materials' bandgap is larger, which may require a larger electric field strength or longer wavelengths to drive LZSM interferometry (see Box 1).

Recent Progress in Theoretical Modeling of Petahertz-fast Ballistic Current Injection

The microscopic description of the generation of petahertz currents in solids is still in its infancy. Within the last years, various theoretical models have been developed to describe the generation mechanism of the CEP-dependent petahertz current in solids. This includes the time-dependent Dirac equation [86, 87], TDSE model simulations ~~(see Fig. 3 a with waveform-dependent asymmetry in the conduction band population)~~ [30, 85, 88], semiconductor Bloch equations [89], ab initio simulations [90, 91] and real space simulations without [92] and with contact electrodes [43, 93]. These simulations can capture the complex electric field dependence (see Fig. 3 **e** and **f**), the polarization dependence [44] and electronic dephasing [94]. However, reproducing the amplitude of the measured charge density is challenging as the charge propagation after injection and charge detection at the interfaces exceed current model simulations.

Recent theoretical studies and initial experimental demonstration highlight that quantum materials with long coherence times or high nonlinearities, such as transition metal dichalcogenide monolayers (TMDC) [85], organic superconductors [62], topologically protected materials [95], Weyl materials [96], or bilayer graphene [97, 98] are promising candidates for future petahertz electronics. In particular, advanced electron control schemes become possible when combined with temporal pulse shaping [99–101], and polarization control [102]. This includes access to spin-, valley-, and Hall-currents [47–50, 103–105]. Furthermore, vectorized electronics [106], and structured light [107] provide additional tools for generating arbitrary superpositions of orthogonal current modes, demonstrating the potential for reconfigurable 'virtual' optoelectronic circuits [108]. In particular, when combined with vectorial optoelectronic metasurfaces, local directional charge flows are generated in condensed media around symmetry-broken plasmonic nanostructures [109].

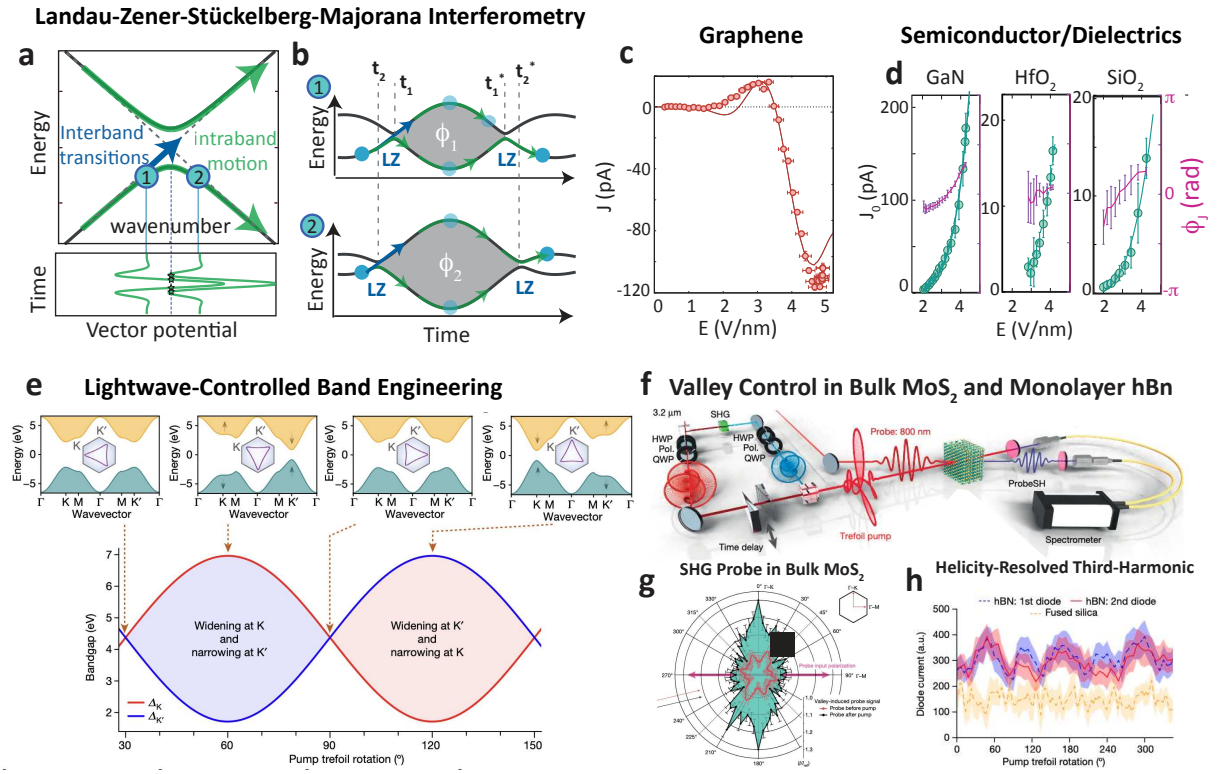

FIG. 3. **Coherent Control in Condensed Matter.** **a**, Under a strong light field, electrons undergo coupled intraband motion and interband transitions (Landau-Zener transition, LZ). In the coherent limit, the LZ transition splits the Bloch electron wavefunction into conduction (CB) and valence band (VB) states, which interfere at subsequent LZ transitions [30, 33, 85]. **b**, For an asymmetric vector potential $A(t)$, i.e., $\varphi_{\mathrm{CE}} = \pi/2$, the phase evolution (gray-shaded) differs for an electron starting at $-k_0$ (marked with label 1) or $+k_0$ (marked with label 2), which may result in an asymmetric residual CB population. **c**, Experimental demonstration of light-field-driven LZSM interferometry in graphene. The CEP-dependent current is measured as a function of field strengths. Current reversals at around 2 and 3 V/nm indicate light-field-driven LZSM interferometry. Figure taken from [35]. A tight-binding model simulation reproduces the current, particularly for field strengths above 3 V/nm, including the current reversals (solid line). **d**, CEP-dependent current as a function of electric field strengths for semiconductor and dielectric materials. Adapted from [38]. **e, Lightwave-controlled valley-selective bandgap modification. An intense light waveform resembling a trefoil structure on the lattice plane is used to coherently manipulate the band structure (shown for hBN). As the field and its vector potential rotate in space, the band structure changes, causing the effective bandgap to oscillate. Figure taken from [49] f, Experimental setup to generate trefoil laser waveforms, which are then applied with an additional probe pulse to bulk MoS_2 or hBn [50]. g, Second harmonic generation (SHG) in bulk MoS_2 with and without prior band engineering (valley polarization) [50]. h, Helicity resolved third harmonic generation in HBn as a signature of band engineering and valley polarization control in hBN [49].**

Lightwave Band Engineering and Valley Control

Petahertz electronics aim to control charge carrier dynamics in materials at sub-cycle speeds of the lightwave for petahertz information processing. Beyond speed, encoding information as classical bits within quantum correlations in materials may open the door to lightwave-based information storage. The recently demonstrated subcycle-controlled, non-resonant valleytronics is an interesting prospect in this direction [49, 50]. Thereby purpose-tailored and intense lightwaves in the order of ∼V/nm are applied to control the spatial-inversion and time-reversal symmetries in solids, which allows unprecedented control over magnitude, location and curvature of the bandgap, i.e., to engineer the material properties, including those not found in pristine materials. The threfoil control field induces complex second-neigbour hopping, which breaks the time-reversal symmetry and lifts the valley degeneracy. For instance, trefoil laser pulses, produced by mixing counter-rotating two-color laser fields, can break the time-reversal symmetry and lifts the valley degeneracy in hexagonal boron nitride (hbN) or bulk MoS_2 [49, 50, 103, 110]. As the field and its associated vector potential rotate in space, the band structure is modified, causing the effective bandgap to oscillate with the rotation of the trefoil light field. This may leads to varying electron excitation dynamics between the valleys as shown in Fig. 3e and a valley polarization. Using a pump-probe setup (3f), the underlying valley polarization is then probed via a subsequent probe pulse. This includes angle resolved second harmonic generation (3g) [50] or via measuring a non-zero Hall current, which create an elliptical third-harmonic signal with valley-dependent helicity (3h) [49]. Lightwave-controlled band engineering holds promises for subfemtosecond-controllable and reversible control of material properties and valley-based information storage and readout.

Based on these recent demonstrations a light-driven alternative to twisted layer stacking has been suggested. By patterning the light wave so that the trefoil shape rotates spatially along the beam profile, micrometre-sized domains with varying electronic properties can be created in the material, similar to Moiré patterning [49].

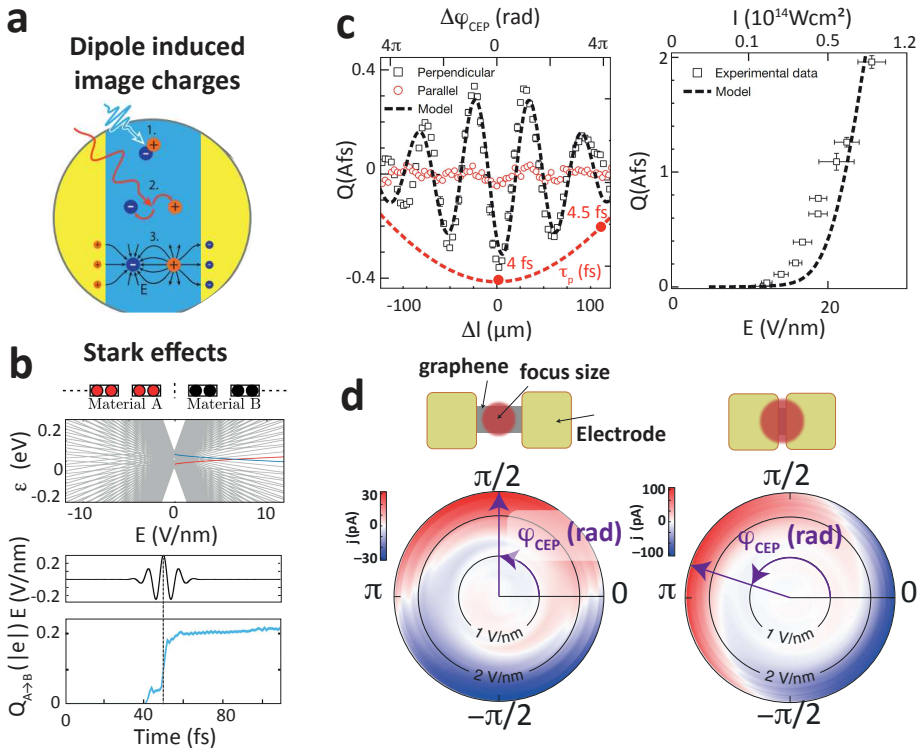

FIG. 4. **Light-Field Electron Dynamics at Material Interfaces.** **a,** Current generation via dipole-induced image charges in condensed media coupled to interfaces. Figure taken from [111]. **b,** Laser-induced electron tunneling across interfaces through Stark shifts. Top panel: The laser-dressed eigenenergies of the heterojunction fan out as E_0 increases, resulting in multiple avoided crossings. Avoided crossings between levels that belong to different materials, such as that signaled by the colored lines, open pathways for electron transfer. Bottom panel: Sub-cycle charge transfer dynamics from material A to B induced by the electric field. Figure adapted from [112]. **c,** CEP-dependent current generation at a metal-dielectric-metal interface (case 2, in Fig. 2). Measured current as a function of CEP (left panel) and highly nonlinear electric field dependence (right panel). **d,** CEP-dependent current generation in a metal-graphene-metal interface with and without interface illumination. The CEP is modulated, and the current response is measured. In the polar plot, the angle represents φ_{CE}, the radius E_0, and the color is the amplitude of the CEP-dependent current. Upon bulk illumination, the current is maximized for interface illumination, and the residual current peaks for $\varphi_{\mathrm{CE}} = \pm\pi/2$, whereas for interface illumination, it peaks close to $\varphi_{\mathrm{CE}} = [0, \pi]$. Figure adapted from [35].

The speed performance of future solid-state electronics systems not only relies on ultrafast current injection, discussed in case (1), but it also requires that the current detection is as short in time as possible and has the broadest possible signature in the frequency domain. In particular, the bandwidth of the measured electronic signal should reach petahertz band-

width, as illustrated in Box 1 **b**. A promising route for petahertz electronics is light-field driven charge generation at material interfaces, as illustrated in Fig. 2 **a**, case (2) **Material Interfaces**, where the current is directly generated at the interface.

Light-field induced currents at interfaces include experiments where the light field generates a dipole in the condensed media, which induces image charge or currents at the interface [111], as shown in Fig. 4 **a**, or experiments where the light field directly modifies the interfacial band alignment via the optical Stark effect and induce a charge transfer on a sub-cycle timescale [93, 112], shown in Fig. 4 **b**.

The first experiment on petahertz-fast electron control at interfaces has been performed by Schiffrin et al., where a gold-silica-gold nano-junction with an electrode distance of 50 nm has been exposed to a strong electric field of a CEP-stabilized 4 fs laser pulse [26]. The lightwave-sensitive current was measured by changing φ_{CE} and the electric field strength E (Fig. 4 **c**).

Since the charge carrier dynamics during the light-matter interaction depends on a highly non-equilibrium state of matter, several microscopic models have been proposed to explain the origin of the CEP-dependent current in case (2). These models include coupling of optical-field-induced charge carriers in condensed media to interfaces [74], as illustrated in Fig. 4 **a**, Zener band-to-band tunneling, field-induced insulator to metal transition of dielectrics through Stark shifts [26, 82, 113–115], Stark control of electrons across interfaces [112, 116–118] (illustrated in Fig. 4 **b**), and resonant and off-resonant quantum path interference processes [119, 120]. Chen et al. developed a state-of-the-art atomistic simulation (time-dependent non-equilibrium Green's function) of the laser-induced time-dependent electronic transport in the nanojunction to find the dominating current generation mechanism for a given system and laser parameters [93]. Contrary to previous simulation and interpretation efforts, this model explicitly considers the role of metallic contacts in the emergence of CEP-dependent current. More recently, screening, band bending, and decoherence are included in model simulations [118, 121, 122]. These simulations recover the experimental observations, i.e., their CEP- and field strength dependences, and indicate that the laser field induces Stark shifts at the interface, which drives charge carriers across the interface on a sub-cycle timescale plays a vital role at material interfaces.

Due to computational costs, these atomistic simulations assume that the laser field is a plane wave that illuminates the interface and the solid equally [93], which is a good approx-

imation when the laser focus is larger than the electrode separation. For larger electrode separations, locally induced transient currents in the condensed media might directly couple to the interface to generate a measurable current (Fig. 4 **a**). Such a current can be used in electric field streaking experiments [53], as discussed in Sec. III. To the best of our knowledge, in this regime, real space calculations, including the coupling to the electrodes and screening, are missing and need to be developed to engineer material interfaces for efficient and fast current generation.

To directly compare the role of the interface with the solid current injection, i.e., case (1) and (2), a metal-graphene-metal interface with variable electrode distances has been illuminated with CE-phase controlled laser pulses (Fig. 4 **d**) [43]. By modulating φ_{CE}, it was found that for pure graphene illumination, i.e., when the electrode distance is larger than the diameter of the focused beam, the current peaks for $\varphi_{\mathrm{CE}} = \pm\pi/2$, i.e., when the vector potential break the inversion symmetry. In contrast, when the interface becomes illuminated, more current is obtained for $\varphi_{\mathrm{CE}} = [0, \pi]$, evidencing the two different current generation mechanisms in (1) and (2).

3. Nanostructured Systems

Over the past 20 years, metallic needle tips subjected to intense and well-controlled lightwaves have been shown to emit electrons on ultrafast and also subcycle timescales of the driving laser, see Box 1 and [10, 13, 14, 75, 123–127]. Inspired by these results, researchers developed on-chip nanostructured elements for lightwave electronics, as shown in Fig. 5 **a**. With their ability to confine and enhance local electric fields at the tip apex, these nanostructures not only enable the generation and control of petahertz-electronic signals using significantly lower incident optical pulse energies than in cases (1) and (2), see Fig. 2 **b**; they also facilitate access to the full toolbox of cleanroom fabrication to come up with smaller and more complex structures for future free electron lightwave electronics circuitry [128].

Building on these findings and continued refinement, it has been demonstrated that the entire structure consisting of the laser-driven emitter, propagation channel, and collector can be fabricated on a single chip [13, 14, 17, 19, 22]. Light-field driven electron emission has now been demonstrated within large-scale arrays of silicon needle tips [129], plasmonic antenna arrays [15, 130, 131], and electrically-connected nanoantenna elements [13, 17], as

shown in Fig. 2 **e**. Using micro- to nanoscale free-space channels, it has further been shown that lightwave-driven electron emission can be maintained in these structures under ambient conditions [13, 14].

Further work has continued to confirm the operation of these devices in the field-driven regime ($\gamma < 1$), as observed from extended needle tips [22], and sub-cycle emission dynamics [75]. Moreover, attosecond field emission from extended needle tips has been measured to (710±30) as [132] and down to (53±5) as [133], demonstrating available bandwidth far in excess of 1 PHz. Mirroring prior developments in high-frequency electronics in the gigahertz to terahertz range, electrically connected nanoantenna arrays have now been used to inject and propagate signals of up to tens of terahertz across millimeter-scale distances on a chip [21], and to provide compact optical-field sampling and phase detection [17–19] as important milestones towards pushing electronic device technology into the terahertz and ultimately petahertz frontier.

However, there are clear challenges that remain. Chief among these challenges are damage and device performance degradation. Metallic structures are more prone to damage due to heating and electromigration effects, which reshape or even ablate the structures [134]. Even slight reshaping of the devices can alter their optical properties, reducing efficiency [17]. Other material candidates with increased tolerance to intense fields and heating could offer a solution. For instance, silicon nanostructures [129] and carbon nanotubes [135] have both demonstrated promise as light-field driven electron emitters. Furthermore, while operation in ambient air alleviates the need for vacuum housing, it also appears to come at a cost: In similar nanoscale vacuum emitters, it has been shown that surface adsorbates from the air lead to reduced emission rates, with vacuum operation resulting in an order of magnitude increase in emission rates with all other conditions held fixed [136]. Similar adsorbate formation is expected to occur in the field-driven regime and is likely another contributing factor to reduced performance over long operation times that has been observed [14, 17]. Potential solutions might be using vacuum packaging or hybrid devices that combine metallic nanostructures and nanoscale dielectric channels [19].

III. APPLYING PETAHERTZ ELECTRONICS: FIELD-RESOLVED OPTICAL DETECTION

Our understanding of strong-field light-matter interactions is fundamental to the continued development of lightwave electronics. Few-cycle, light-matter interactions are often highly nonlinear in nature and are sensitive to the precise shape of the optical field waveform in time, not just to the cycle-averaged intensity envelope. As a consequence, understanding these interactions requires precise knowledge of the shape of the exciting optical field waveform. Unfortunately, the measurement of few-cycle tailored waveforms, particularly those in the fJ to pJ energy range, has remained challenging using conventional optical detection methods.

Typical techniques for optical pulse characterization operate in the frequency domain and use numerical retrieval algorithms [137]. Experimental challenges arise from the large bandwidths of few-cycle pulse retrieval, which often approach or exceed one octave of bandwidth [72]. These challenges include phase-matching constraints and difficulties in background removal due to spectral overlap of the fundamental and up-converted frequencies involved in the measurement process. Furthermore, these challenges create difficulties for the needed pulse retrieval algorithms, which require accurate models of the measurement process.

Similar to the symbiotic relationship between nanoscale science and nanoscale technologies, we are developing better tools for field-resolved optical detection as we better understand the strong-field interactions underlying petahertz electronics. These techniques operate directly in the time domain where the fields are short-lived, removing the need for more complicated broadband spectroscopic analysis. By implementing lightwave-electronic techniques in solid-state systems, we are also seeing orders of magnitude reductions in needed pulse energies for petahertz-electronic CEP detection and field sampling (see Fig. 3b and Ref. [138]). In particular, through the use of nanoscale enhancement structures, it is possible to achieve petahertz-scale currents with just tens of picojoules of pulse energy [13, 75], enabling field-resolved waveform sampling down to the femtojoule-level [18].

Below, we briefly highlight key results in using concepts and petahertz electronics for CEP detection and optical field sampling.

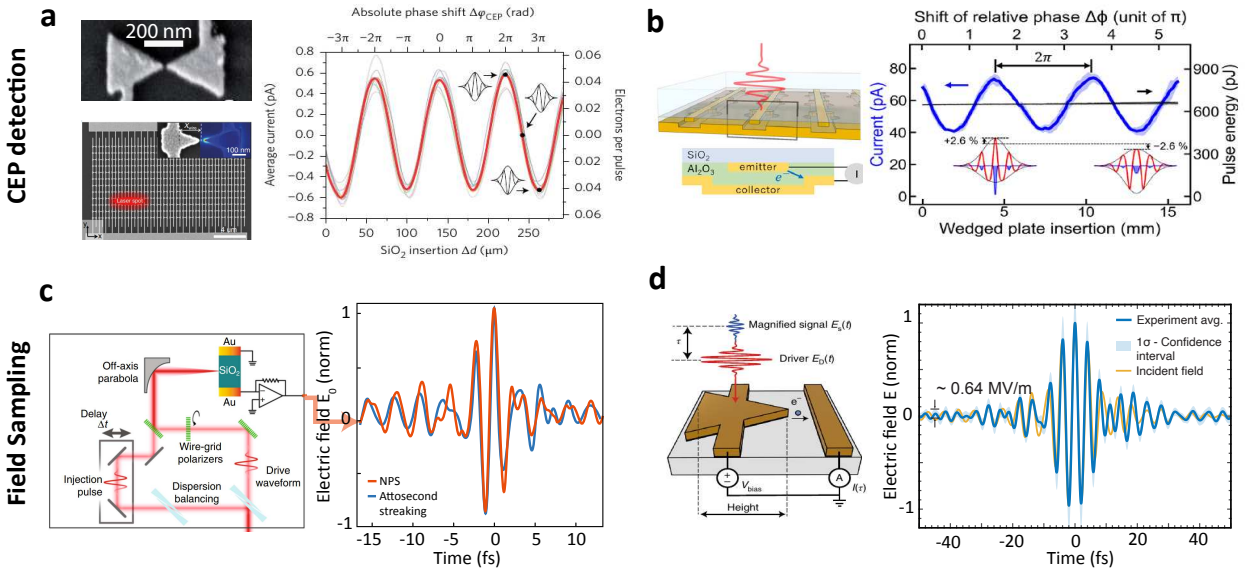

FIG. 5. **Carrier-Envelope Phase Detection and Sub-Cycle Optical Field Sampling with PHz Electronics.** **a-b**, Representative works demonstrating CEP-sensitive electron emission in petahertz electronic systems. **a**, CEP-dependent current emission from electrically-connected plasmonic bow-tie antennas. A picoampere-level CEP-dependent current is generated in a single antenna pair using picojoules of pulse energy. Figure replotted from Ref. [13]. **b**, CEP-detection in hybrid devices. The metal antennas were embedded within a dielectric, creating a hybrid nanoantenna and dielectric system to reduce damage compared to air gaps. Adapted from Ref. [19]. **c-d**, Demonstrations of optical field sampling using petahertz electronics. **c**, Sampling of few-cycle waveforms using streaking-based methods in silicon dioxide. Adapted from Ref. [53]. **d**, Perturbative sampling using plasmonic nanoantenna arrays, with energy sensitivity below 5 fJ, and field sensitivity down to 0.64 MV m^{-1}. Adapted from Ref. [18].

1. *Carrier-Envelope Phase Detection*

Optical-field control of electrons in nanostructures [13, 14], within dielectrics [26] and two-dimensional materials [44] have been shown to exhibit a CEP-sensitive response in the few-cycle regime. The CEP-sensitive response can manifest as modulation of the emitted photocurrent (see Figs. 5 **a, b** and Box 2).

This was observed early on in strong-field electron emission from metal surfaces [139] and the generation of sub-cycle currents within dielectrics [26]. While these initial demonstrations of CEP-sensitive photocurrents required large pulse energies (micro-Joule-level), recent work has shown that nanoscale field-enhancement structures can be used to reduce the needed pulse energies by orders of magnitude (pico- to nano-Joule-level) [13, 14], and arrayed to generate increased photocurrents [17]. Building on these findings, recent results indicate

the possibility of shot-to-shot readout for CEP tagging using only nanojoules of pulse energy in the mid-infrared to generate more than 1000 CEP-sensitive electrons per laser shot (2.7 µm central wavelength) [140]. Calculations show that such detection techniques could compete with comparable f-$2f$ CEP detection methods in integrated photonics [141].

Advancements in phase-resolved waveform detection combined with nanostructures allows for phase-resolved measurements of broadband focused few-cycle pulses in the near and far field, including the Gouy phase [142–144], and build-up and dephasing of the plasmonic excitation near metallic objects [145]. With time, chip-scale petahertz electronics could provide a flexible and integrated alternative for CEP detection featuring shot-to-shot readout at low pulse energies without the need for nonlinear conversion or interferometric detection.

2. Sub-Cycle Optical Field Sampling

By generating sub-optical-cycle electronic currents, it is possible to stroboscopically measure the fields of light as they oscillate in time. These methods were first pioneered using atomic and molecular systems. For example, in attosecond streaking, an attosecond EUV pulse excites a free electron from an atomic system in the presence of a longer-wavelength optical streaking waveform [4, 146]. A delay-dependent momentum shift of the emitted electron then records the vector potential of the optical streaking wave in time. More recently, a method known as tunneling ionization with a perturbation for the time-domain observation of an electric field (TIPTOE) was demonstrated [147, 148]. In TIPTOE, highly nonlinear photoemission from an atomic or molecular gas driven by a strong gate waveform emits sub-cycle electron bursts. A weaker signal waveform then perturbs the generation of these bursts, providing a direct measurement of the signal waveform in time as the delay between the signal and gate is scanned. **Similarly, photo-assisted electron tunneling in nanoantenna junctions has been used to sample broadband optical fields [20, 149].** These streaking and perturbative waveform sampling techniques, being the most commonly used, have now been translated to the chip scale using petahertz electronics. See Box 2 for a complete description of the fundamental principles behind streaking and perturbative techniques in petahertz electronics. We note that there are various other optical field sampling techniques, such as electro-optical sampling or generalized heterodyne

optical-sampling technique (ghost) [150]; here, we focus on chip-scale current-based detection schemes and refer for further review to [138].

In Schiffrin *et al.* [26] a streaking-like method was introduced whereby sub-cycle charge bursts were generated by a strong gate field driving nonlinear currents between the valence and conduction bands of SiO_2. These sub-cycle charge bursts were then streaked within the SiO_2 by an orthogonally-polarized signal field (see Box 2). Like in attosecond streaking, the momentum of these excited charges was modulated by the cross-polarized signal field as a function of the delay between the signal and gate, resulting in a delay-dependent current proportional to the vector potential of the signal $A_s(t) = \int_t^\infty E_s(t')dt'$. This method is often referred to as nonlinear photoconductive sampling (NPS). A typical result of field sampling using NPS is shown in Fig. 5 **c** (adapted from Ref. [53]). In addition to NPS, a related technique known as linear photoconductive sampling (LPS) can also be used where the injected charge bursts within the dielectric result from the linear photoabsorption of a sub-cycle burst of high-energy photons, such as extreme ultraviolet pulses from high-harmonic generation. In the last decade, these streaking-like techniques within solid-state media have been studied extensively, demonstrating the ability to measure optical waveforms spanning from the mid-infrared down to ultraviolet wavelengths [26, 56, 106, 151]. Important to the continued development of petahertz electronics, the LPS technique was recently used to quantify the fundamental speed limit of high-bandgap optoelectronics [111], which was determined to be on the order of 1 PHz.

Analogous to the TIPTOE approach in gas-phase media, perturbative approaches to sub-cycle field sampling in the visible to near-infrared have now also been demonstrated (see Box 2). In these techniques, sub-cycle current emission driven by a strong gate waveform in a solid-state system is modulated by a weak signal waveform as a function of delay. For a short-enough gate pulse, the delay-dependent photocurrent is in one-to-one correspondence with the time-domain shape of the electric field of the signal waveform $E_s(t)$. This direct readout of the signal's electric field differentiates these perturbative techniques from streaking-like techniques such as NPS and LPS which measure the signal's vector potential $A_s(t)$. While in theory it is trivial to convert from the vector potential to the electric field, there are consequences for realistic signals, such as derivative-induced noise in converting $A_s(t)$ to $E_s(t)$.

There have now been several demonstrations of perturbative field-sampling methods using

solid-state and on-chip systems. These include the all-optical sampling of infrared pulses in solids [54], single-shot sampling of few-cycle mid-infrared waveforms using silicon CCD arrays [152], polarization-resolved sampling of vortex fields using optical tunneling from needle tips [55], and the sub-cycle sampling of femtojoule-level few-cycle waveforms in the near-infrared [18] (see Fig. 5 **d**). **Furthermore, advances in waveform detection, such as using dual frequency combs [153, 154] allow for delay calibration down to the few-attosecond precision with picosecond delay ranges. Also, two slightly carrier-frequency-shifted laser pulses have been applied to sample arbitary waveforms with broad spectral bandwidts as well as localized surface plasmons in metallic nanostructures [20, 149]**.

In electronics, access to oscilloscopes allowed the real-time measurement of electrical signals and their waveforms, which was crucial for advancing electrical signal processing and communication. Similarly, access to the time domain at optical frequencies via analog petahertz electronics opens various opportunities, such as direct access to electrons, phonons, and many-body particle motion in real time. A better understanding of light-matter interaction in the time domain, such as exciton and charge-transfer dynamics, is essential for efficient photovoltaics, coherent control of chemical bonding and dissociation, and may find ramifications in biological sensing and analysis [155].

Box 2: Perturbative vs. Streaking-Based Sampling with Petahertz Electronics

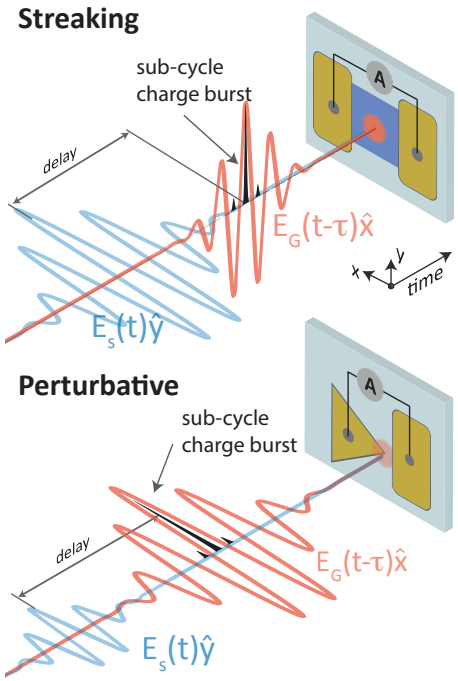

Streaking vs. Perturbative Field-Sampling Approaches. ***top****, Streaking-based approaches use cross-polarized gate and signal waveforms. The gate waveform (red) excites sub-cycle charge bursts (shaded regions) that are then pushed and pulled to contacts on either side by the signal fields (blue). This results in a delay-dependent measurement of the vector potential of the signal field.* ***bottom****, For perturbative approaches, the emission rate itself is perturbed. The sub-cycle charge bursts (shaded regions) driven by the gate (red) are modulated in their strength by some weak signal field (blue). This results in a direct modulation of the output emission current which replicates the signal fields.*

Methods for time-domain sampling using petahertz electronic systems can be divided into two categories: streaking and perturbative sampling. Examples are both shown pictorially in the figures above. Both work by exciting a petahertz electronic device using two pulses: a relatively strong gate pulse E_{G}, and a weaker signal pulse E_{S}. The delay between these two pulses is scanned, which then modulates the current response emitted. This emitted current modulation encodes time-domain information about the signal pulse.

For streaking techniques, the gate and signal are cross-polarized, as shown in the top panel. The gate field excites an electron emission response within a solid-state medium (shaded curve). The emitted electrons are then pushed or pulled by the signal field towards one of two contacts (see picture of dielectric on the right with two metal contacts). One can write the delay-dependent current response as

$$I_{\mathrm{streak}}(\tau) \propto \int_{-\infty}^{\infty} \mathrm{d}t A_{\mathrm{s}}(t) G_{\mathrm{streak}}(t-\tau) \tag{2}$$

where I_{streak} is the measured current, $A_{\text{s}}(t)$ the vector potential of the signal field in the Coulomb gauge, and $G_{\text{streak}}(t)$ is the impulse response of the streaking process. Given a sufficiently short $G_{\text{streak}}(t-\tau)$ the measurement converges to the vector potential of the signal field such that $I_{\text{streak}}(\tau) \propto A_{\text{s}}(\tau)$. Note that one can then find the electric field of the signal through differentiation as $E_{\text{s}} = -\frac{\partial E_{\text{s}}(t)}{\partial t}$.

For perturbative approaches, both fields are polarized in the same direction, and the emission rate is modulated by the signal field. The process is summarized in the bottom panel. A strong gate field drives a nonlinear, sub-cycle electronic response within a system (here, we take emission from a nanoantenna as an example similar to Ref. [18]). This sub-cycle emission response is perturbed by some weak signal field that is phase-locked to the gate field. The oscillating readout signal as a function of delay between the signal and gate is then

$$I_{\text{pert}}(\tau) \propto \int_{-\infty}^{\infty} \mathrm{d}t E_{\text{s}}(t) G_{\text{pert}}(t-\tau) \tag{3}$$

where I_{pert} is the measured signal (e.g., current or fluorescence), $E_{\text{s}}(t)$ the signal electric field, and $G_{\text{pert}}(t) = \frac{\partial \Gamma}{\partial E}|_{E_{\text{gate}}(t)}$ the impulse response of the process with Γ the field-driven electronic response.

Given a sufficiently sub-cycle $G_{\text{pert}}(t-\tau)$ the signal corresponds to the electric field of the signal such that $I_{\text{pert}}(\tau) \propto E_{\text{s}}(\tau)$. Unlike streaking methods, perturbative methods provide a direct measurement of the electric field. They also do not require isolated sub-cycle electronic transients, enabling field sampling through multicycle gate fields. It should be noted, however, that this is at the cost of CEP-sensitivity and response bandwidth, which does require a few-cycle gate field to generate an isolated electronic transient (see Refs. [18, 148].

IV. OUTLOOK: TOWARDS ON-CHIP DIGITAL PETAHERTZ ELECTRONICS.

Within the last ten years, light-field control of electrons in the petahertz range has evolved from bulky and complex gas phase experiments with high-power lasers at low repetition rates to compact petahertz electronics in solids and nanostructures driven with high repetition rate picojoule laser oscillator systems. Applications of petahertz electronics are still in their infancy and have mainly been limited to CEP detection, electric field sampling, and switching, thus representing the *analog age of petahertz electronics*. Yet, recent simulations and initial experimental demonstrations propose first classical and quantum logic operations [43, 45, 128, 156], and memory functionality [45, 128], controlled at optical frequencies. This section provides an ~~overview of~~ **outlook based** on ongoing theoretical and experimental efforts toward digital petahertz electronics.

Petahertz Memory and Logic Devices: Building on petahertz-fast current injection in dielectrics, as discussed around Fig. 2, rectification (diode) [156] and memory operation (four-bit data RAM) [45] has been proposed in dielectric heterostructures. For this, a laser pulse injects charge to the heterostructure (write pulse), which is stored in a capacitor and read by a second laser pulse. Similarly, but instead of a dielectric heterostructure, a circuit consisting of triangular antenna-diode pairs and a storage capacitor (Fig. 6 **a**) was proposed in Ref. [128]. Based on model simulations, such an ultrafast memory cell, which uses optical pulses as read and write signals, shows memory operations at frequencies beyond 100 THz. **As a future prospective, these bow-tie nanoantennas may be coupled to a waveguides to directly interact with few-cycle supercontinuum light sources allowing for fully-integrated frequency comb stabilization and lightwave-based petahertz electronics [157].**

Logic operations controlled by the shape of two incident light fields have been demonstrated in a graphene device [43]. The underlying logic builds on the waveform-dependent current generated by both bulk and interfacial charge carriers (discussed in Sec. II B 1 and II B 2). Using two incident light pulses with varying pulse shapes, assigned to logic inputs of zero or one, it has been demonstrated that the total current yielded the logic output. Depending on the pulse shapes and the input bit encoding, the device exhibits behavior characteristic of ultrafast logic AND, OR, NAND, and NOR gates.

Arbitrary waveform generators at optical frequencies: To control the current generation process precisely, and to ultimately perform computation, it is essential to synthesize the appropriate driving lightwaves, similar to the arbitrary waveforms generated routinely at radio and microwave frequencies (Fig. 6 **b**) [51]. For this, multi-octave broadband and phase-stable laser sources have been demonstrated, covering the spectral range from THz to UV [158, 159]. These sources provide a platform for tunability beyond CEP-control and represent the first steps towards arbitrary waveform generators at optical frequencies [72, 160, 161]. Applying these pulses to solids and nanostructures will allow us to excite (write), manipulate, and read quantum states within a single laser pulse.

So far, most petahertz electronic demonstrations rely on external laser sources focused on the sample. On-chip mode-locked laser sources and integrated nonlinear photonics have

recently demonstrated the capability to generate 10-gigahertz on-chip high-power few-cycle laser pulses [162, 163], supercontinuum generation for frequency comb generation [164] and on-chip power distribution [165]. Together with these advances, carrier-envelope offset detection [143, 166], and the first fully integrated plasmonic nanostructures coupled to Si_3N_4 core waveguides for CEP detection inside waveguides have been proposed [157], paving the path for all on-chip petahertz metrology and electronics.

Petahertz Quantum Logic Gates: Quantum logic gates are fundamental building blocks of quantum circuits, the quantum analogs of classical digital circuits. In classical computers, information is processed using bits that can be either 0 or 1. Quantum computers, on the other hand, use qubits, which can exist in a coherent superposition of states, representing both 0 and 1 simultaneously. Quantum logic gates are operations that coherently manipulate the state of qubits to perform quantum computations, with common quantum logic gates such as the NOT, Hadamard, CNOT, and SWAP gates. These gates are often realized via resonant driving, resulting in Rabi oscillations. Increasing the frequency of operation and, thus, an increase in the number of operations within the coherence time of the system requires an increase in the Rabi frequency. This is directly linked to an increase in the strength of the electric field. This, however, presents several challenges, such as interaction with other states or increased environmental noise [167]. To overcome these limitations, very recent works suggested off-resonant driving of qubits to increase the speed performance [167, 168]. The underlying processes can be understood based on the framework of sub-cycle Landau-Zener-Stückelberg-Majorana (LZSM) transitions [169], as we have discussed in Sec. II B 1. Figure 6 **c** illustrates the basic mechanism of LZSM-driven quantum gates. The coherent superposition states of input state E_i are modified via LZ transitions. In Ryzhov et al. [167], the field-driven dynamics of a multilevel quantum system under LZSM drives are explored, and the optimal parameters for certain logic quantum operations are presented. Figure 6 **d** and **e** show the response of a 2-qubit system under optimized parameters for an iSWAP gate.

While controlled quantum superposition (LZSM transitions) in qubits has been demonstrated up to a driving frequency of 10 GHz (see Table 1 in [169]), petahertz control of quantum logic gates has not been experimentally demonstrated. The recently demonstrated sub-cycle driven LZSM interferometry in graphene certainly bodes well for this feat [30, 44]. While the electrons in graphene are delocalized and thus have a short coherence time [94],

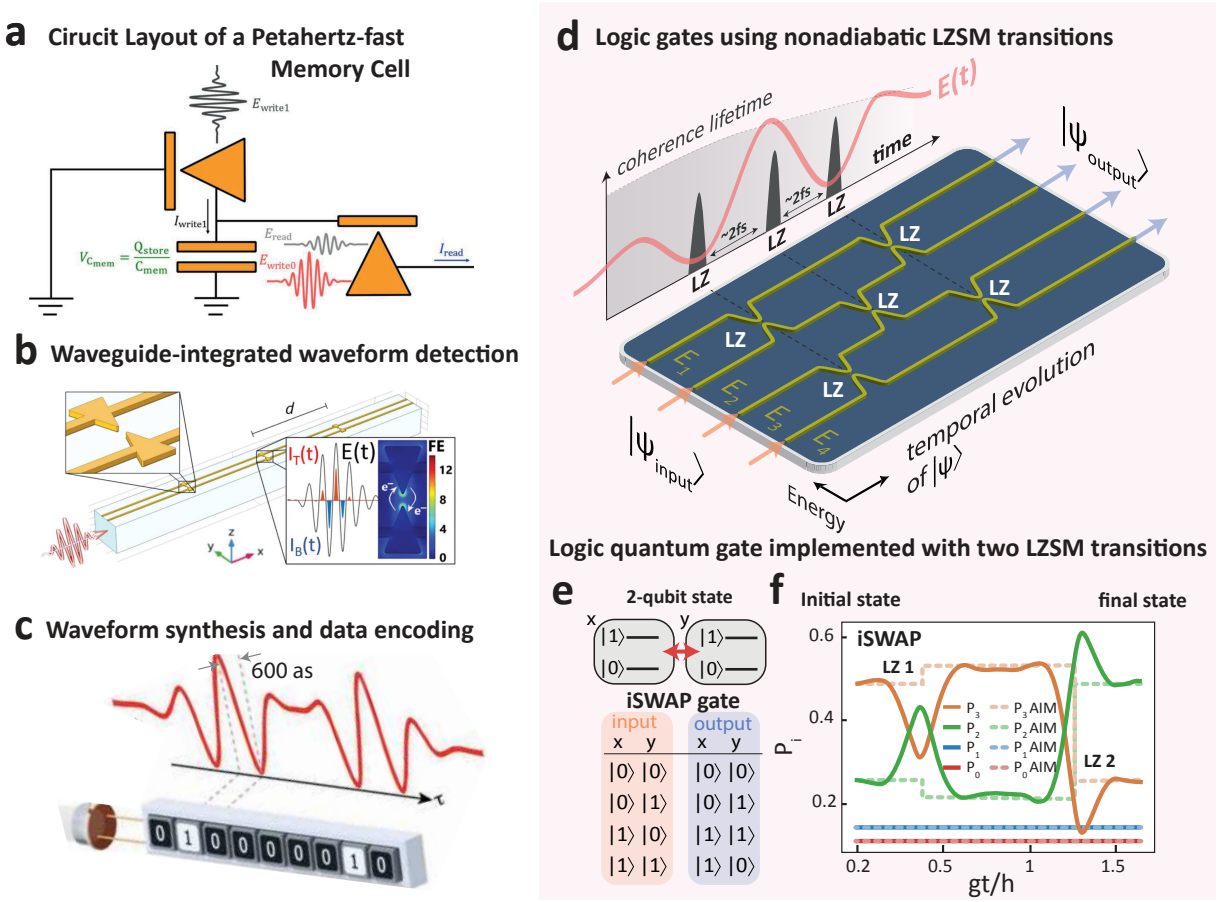

FIG. 6. **On-Chip Petahertz Electronics.** **a,** Circuit layout of an ultrafast memory cell using two triangular antenna diode pairs and a storage capacitor. Figure adapted from [128]. **b,** To-scale schematic of electrically-connected bow-tie CEP detectors integrated onto a Si3N4 waveguide. Figure adapted from [157] **c,** Data encoding on synthesized light fields. Figure adapted from [51]. **d,** Temporal evolution of multiple quantum states $|\Psi_{\text{input}}\rangle$. The superposition of these states can be coherently controlled via subsequent Landau-Zener (LZ) transition, as proposed in [167]. These LZ transitions are induced by synthesized lightwaves, allowing for sub-cycle, fs-fast coherent control. **e,** The truth table of the quantum logic iSWAP gate, consisting of two coupled qubits, is shown. **f,** Example of optimized driving parameters to achieve an iSWAP gate via two LZ transitions. The occupation probabilities P_i of each adiabatic level E_i as a function of time are obtained by two methods: numerical solutions of the Liouville-von Neumann equation (solid line) and by the adiabatic-impulse model (dashed line). Figure adapted from [167].

localized electrons, such as found in quantum dots, defect states, or Moiré excitons, might enable a longer coherence time. Furthermore, while most quantum operations require low temperatures to improve the system's coherence, the coherence time requirement can be relaxed by controlling the system at optical frequencies, ultimately enabling quantum operations at room temperature.

Strong-field Petahertz Quantum Information Processing:

The ability to manipulate materials at petahertz speeds, faster than electronic decoherence enables the coherent control and read on the level of a single electron wave function, even at room temperature. Combined with lightwave band engineering and the discovery and utilization of novel quantum states, in particular in quantum materials with intrinsic correlations may further provide new avenues for novel information storage and quantum-based applications and technologies.

Grand Challenges Towards Integrated Petahertz Electronics at High Repetition Rates:

Despite recent advances in controlling currents within solids and nanostructures at petahertz bandwidths, several challenges must be addressed to achieve integrated petahertz electronics. These challenges include the development of potential communication strategies and data encoding at optical clock rates, chip integration and conversion between electronic and optical information, including interfacing to conventional high-bandwidth circuits. The technological progress to gigahertz electronics has been largely enabled by improvements in integration, miniaturization, and material and device interfaces, leading to the application of higher electric field strengths, and thus faster control over currents. Similarly, advances in material interfaces, integration and plasmonics can lead to more efficient power generation at optical frequencies (see Fig. 1). While initial developments in petahertz electronics have focused on the speed of current excitation, as we push to higher and higher repetition rates, femotosecond-scale charge relaxation and readout will also become a critical requirement.

The extent to which these challenges can be overcome to achieve faster computation in practical electronics remains unclear. However, over the past decade, petahertz electronics has made significant strides, particularly in developing petahertz-fast oscilloscopes with great potential for future spectroscopic applications (marking the analog era of petahertz electronics). Additionally, petahertz electronics may hold great promise for quantum-related computation.

V. SUMMARY

The emerging experimental and theoretical tools for lightwave-driven physics in condensed matter enable the manipulation of electron motion and, thus, currents in solids and nanostructures at petahertz frequencies. In this regime, the electrons are controlled by the light wave rather than their photon-based response and on a time scale that allows us to treat them completely coherently, which may become essential for future quantum computation approaches. Furthermore, propelled by the development of compact and high repetition rate laser sources, particularly on-chip photonics, temporally and spatially structured light sources, truly integrated petahertz electronic components are on the horizon. Compared to early experiments in the gas phase, lightwave-driven currents in solids also provide access to material properties, such as spin, valley correlations, topology, magnetism, phase transition, nanostructuring, and engineering on the atomic level, which might provide further tools to enhance the light-matter interaction and shape the future of petahertz electronics.

VI. SUPPORTING INFORMATION

A. Performance Comparison

Here we briefly summarize the efficiency and compactness of the current generation process in cases (1)-(3) (see Fig. 2), and propose a pathway to enhance the efficiency of each scheme.

Firstly, bulk media benefits by having the largest photoactive area, potentially yielding many CEP-dependent photocarriers. Challenges arise, however, as these carriers must traverse the material to reach an interface where charge separation and current generation occur. The inefficiency arises from the possibility of charge carriers recombining and losing momentum before reaching the electrodes. For example, in graphene, it has been demonstrated that the current amplitude scales $1/g^2$, with g the electrode distance [43]. In a similar work and for long electrode distances a $1/g$-dependence has been observed [74]. For petahertz-fast current generation in bulk media, laser pulses with nJ energy levels are used to generate $10^{-4} - 10^{-2}$ fC per laser shot, resulting in an efficiency of $10^{-5} - 10^{-3}$ fC/nJ [30, 32–34, 38]. Note that this efficiency is also directly related to the asymmetry of the laser pulse [34] and its pulse duration. The larger the asymmetry of the laser pulse, the larger the CEP-dependent response (see waveforms in Fig. 2 **a**). Experiments with two-color or close to single-cycle laser pulses yield a larger waveform-sensitive current (see open hexagon in Fig. 2 **c**). Furthermore, we note that experimentally, materials with smaller bandgap yield a higher efficiency, see for example GaN in [36] or [37]

In contrast, direct illumination of interfaces, primarily formed between large bandgap materials (e.g., SiO_2, GaN, Al_2O, CaF_2) and metals, presents a different scenario. These interfaces typically feature a substantial Schottky barrier (several eV [170]), requiring either high electric fields for sub-cycle tunneling via Stark control or efficient dipole coupling (see discussion around Fig.4). Additionally, in cases of light-field-induced Stark control, the photoactive area is reduced to one dimension, which limits the amount of lightwave-sensitive charge carriers generated. Here, $\sim \mu$J laser pulses generate typically around $\sim$10 fC CEP-sensitive charge carriers with an efficiency of$10^{-3} - 10^{-1}$ fC/nJ [26, 36, 37, 39, 40].

Nanostructures exhibit further reduced dimensionality, resulting in a lower waveform sensitive current per device. Nevertheless, the true advantage of nanostructures lies in their ~~plasmonic~~ **capability to produce large** field enhancement**s**. This allows the use of pi-

cojoule and high-repetition-rate laser systems to enter $\gamma < 1$ and obtain $\sim 10^{-5}$ fC CEP-dependent charge carriers with an efficiency of $\sim 10^{-4}$ fC/nJ [13, 17, 75]. Moreover, arranging these compact nanostructures in an array-like structure increases their active area and, thus, their efficiency by 2 orders of magnitudes to $\sim 7.5\times\ 10^{-3}$ fC/nJ [140].

While materials with a large band gap or high work function demand a large local electric field to reach the strong field regime, they offer the benefit of suppressing resonant waveform-independent photocarrier generation. These carriers heat the system, potentially damaging the device.

Potential avenues for increasing the CEP-dependent current include leveraging nanoparticles for local field enhancement in bulk media [171], multilayered materials [172] or patterned electrodes and pn or Schottky-like junctions [173] for more efficient charge collection. Furthermore, increasing the density of nanostructure arrays and strategies to increase the field enhancement via teardrop-like plasmonic nanostructures [109] with field enhancement factors of 60 might further boost the efficiency of hybrid bulk-nanostructure petahertz electronic devices.

Ref.	**System**	$E_{\mathbf{pulse}}$ **[nJ]**	ω_0 **[μm]**	**d [μm]**	j**[pA]**	$j_{\mathbf{pulse}}$ **[fC]**	Q **[fC/μJ]**	λ_0 **[nm]**	τ **[fs]**	$f_{\mathbf{rep}}$ **[MHz]**	E_0 **[V/nm]**
25	Graphene	0,8	1,5	5	17	0,000213	0,266	800	5,5	80	3
27	Graphene	0,7	1,5	4	95	0,00119	1,7	800	5,5	80	2,8
28	Graphene	0,8	1,5	5	40	0,0005	0,625	800	5,5	80	3
29	Graphene	0,7	1,5	10	20	0,00025	0,357	800	5,5	80	3
29	Graphene	0,75	1,8	10	7000	0,0875	117	400/800	5,5	80	3
31	GaN	100	13	5	1600	8	80	800	6,4	0,2	6,2
21	SiO2	8300	50	0,05	6	2	0,241	750	3,8	0,003	20
35	CaF2	15000	50	10	18	6	0,4	750	4	0,003	27
34	Al2O3	10000	50	10	72	24	2,4	750	4	0,003	22
34	SiO2	6000	50	10	144	48	8	750	4	0,003	17
34	CaF2	10000	50	10	57	19	1,9	750	4	0,003	21
32	GaN	1300	50	10	8,4	2,8	2,15	760	3,8	0,003	8
32	GaN	333	50	5	12	4	12	760	3,8	0,003	4
32	GaN	1300	50	0,1	3	1	0,769	760	3,8	0,003	8
33	GaN	0,81	1,8	5	170	0,00213	2,62	800	5,4	80	4,5
33	HfO2	0,81	1,8	5	1,9	0,0000238	0,0293	800	5,4	80	4,5
33	SiO2	0,81	1,8	5	15	0,000188	0,231	800	5,4	80	4,5
12	Nano	0,08	1	0,01	0,6	0,0000075	0,0938	1500	6	80	2,9
138	Nano	80	21	0,05	18,4	0,64	7,5	2700	16	0,05	1
70	Nano	0,021	1,5	0,01	1,78	0,0000124	0,59	1250	4,2	80	1
16	Nano	0,19	3	0,03	14	0,000179	0,945	1177	10	78	1,4
13	Nano	0,16	3	5	1,45	0,0000186	0,116	1177	10	78	NA
164	Nano	1,5	1,7	0,75	1,8	0,0000225	0,015	800	5,5	80	4,8

TABLE I. Summary of parameters used to populate Fig. 2 **b**, and **c** and additional experimental parameters. The device design (bulk material or, nano: nanostructured system), pulse energy E_{pulse}, the beam waist ω_0, the contact electrode distance g, the measured CEP-dependent current j, the charge per pulse Q_{CEP}, the efficiency η, the center wavelengths λ_0, the pulse duration τ, the repetition rate f_{rep} and the applied electric field strengths E_0 are listed. Parameters not directly stated in the publication are best estimates.

ACKNOWLEDGMENTS

We acknowledge fruitful discussions with Peter Hommelhoff. C.H.'s and M.F.K.'s work was supported by the DOE, BES, Chemical Sciences, Geosciences, and Biosciences Division (CSGB). P.D.K.'s work was supported by the National Science Foundation under Grant No. 2238575, and by the U.S. Department of Energy, Office of Science, Office of Basic Energy Sciences, under Award Number DE-SC0024173.

[1] Ambrose Fleming, "Guglielmo Marconi and the Development of Radio-Communication," Journal of the Royal Society of Arts **86**, 41–64 (1937).

[2] M. Th. Hassan, A. Wirth, I. Grguraš, A. Moulet, T. T. Luu, J. Gagnon, V. Pervak, and E. Goulielmakis, "Invited Article: Attosecond photonics: Synthesis and control of light tran-

sients," Review of Scientific Instruments **83**, 111301 (2012).

[3] Robert Boyd, Nonlinear Optics, 3rd ed. (Elsevier Science & Technology, San Diego, California, 2008).

[4] M. Hentschel, R. Kienberger, Ch. Spielmann, G. A. Reider, N. Milosevic, T. Brabec, P. Corkum, U. Heinzmann, M. Drescher, and F. Krausz, "Attosecond metrology," Nature **414**, 509–513 (2001).

[5] P. M. Paul, E. S. Toma, P. Breger, G. Mullot, F. Auge, Ph. Balcou, H. G. Muller, and P. Agostini, "Observation of a train of attosecond pulses from high harmonic generation," Science **292**, 1689–1692 (2001).

[6] P. B. Corkum and Ferenc Krausz, "Attosecond science," Nature Physics **3**, 381–387 (2007).

[7] A. Baltuška, Th. Udem, M. Uiberacker, M. Hentschel, E. Goulielmakis, Ch. Gohle, R. Holzwarth, V. S. Yakovlev, A. Scrinzi, T. W. Hänsch, and F. Krausz, "Attosecond control of electronic processes by intense light fields," Nature **421**, 611–615 (2003).

[8] Sergey Zherebtsov, Thomas Fennel, Jürgen Plenge, Egill Antonsson, Irina Znakovskaya, Adrian Wirth, Oliver Herrwerth, Frederik Süßmann, Christian Peltz, Izhar Ahmad, Sergei A. Trushin, Vladimir Pervak, Stefan Karsch, Marc J. J. Vrakking, Burkhard Langer, Christina Graf, Mark I. Stockman, Ferenc Krausz, Eckart Rühl, and Matthias F. Kling, "Controlled near-field enhanced electron acceleration from dielectric nanospheres with intense few-cycle laser fields," Nat. Phys. **7**, 656 (2011).

[9] Michael Krüger, Markus Schenk, and Peter Hommelhoff, "Attosecond control of electrons emitted from a nanoscale metal tip," Nature **475**, 78–81 (2011).

[10] G. Herink, D. R. Solli, M. Gulde, and C. Ropers, "Field-driven photoemission from nanostructures quenches the quiver motion," Nature **483**, 190–193 (2012).

[11] Stefan A. Maier, Plasmonics: Fundamentals and Applications (Springer US, 2007).

[12] Sebastian Thomas, Georg Wachter, Christoph Lemell, Joachim Burgdörfer, and Peter Hommelhoff, "Large optical field enhancement for nanotips with large opening angles," New Journal of Physics **17**, 063010 (2015).

[13] Tobias Rybka, Markus Ludwig, Michael F. Schmalz, Vanessa Knittel, Daniele Brida, and Alfred Leitenstorfer, "Sub-cycle optical phase control of nanotunnelling in the single-electron regime," Nature Photonics **10**, 667–670 (2016).

[14] William P. Putnam, Richard G. Hobbs, Phillip D. Keathley, Karl K. Berggren, and Franz X. Kärtner, "Optical-field-controlled photoemission from plasmonic nanoparticles," Nature Physics **13**, 335–339 (2017).

[15] Péter Dombi, Anton Hörl, Péter Rácz, István Márton, Andreas Trügler, Joachim R. Krenn, and Ulrich Hohenester, "Ultrafast Strong-Field Photoemission from Plasmonic Nanoparticles," Nano Letters **13**, 674–678 (2013).

[16] J. Schoetz, Z. Wang, E. Pisanty, M. Lewenstein, M. F. Kling, and M. F. Ciappina, "Perspective on Petahertz Electronics and Attosecond Nanoscopy," ACS Photonics **6**, 3057–3069 (2019).

[17] Yujia Yang, Marco Turchetti, Praful Vasireddy, William P. Putnam, Oliver Karnbach, Alberto Nardi, Franz X. Kärtner, Karl K. Berggren, and Phillip D. Keathley, "Light phase detection with on-chip petahertz electronic networks," Nature Communications **11**, 1–11 (2020).

[18] Mina R. Bionta, Felix Ritzkowsky, Marco Turchetti, Yujia Yang, Dario Cattozzo Mor, William P. Putnam, Franz X. Kärtner, Karl K. Berggren, and Phillip D. Keathley, "On-chip sampling of optical fields with attosecond resolution," Nature Photonics **15**, 456–460 (2021).

[19] Ko Arai, Daiki Okazaki, Ikki Morichika, and Satoshi Ashihara, "All-solid-state optical-field-sensitive detector for sub-nanojoule pulses using metal–insulator hybrid nanostructure," ACS Photonics **10**, 1702–1707 (2023).

[20] Yang Luo, Alberto Martin-Jimenez, Frank Neubrech, Na Liu, and Manish Garg, "Synthesis and direct sampling of single-cycle light transients by electron tunneling in a nanodevice," ACS Photonics **10**, 2866–2873 (2023).

[21] Christoph Karnetzky, Philipp Zimmermann, Christopher Trummer, Carolina Duque Sierra, Martin Wörle, Reinhard Kienberger, and Alexander Holleitner, en"Towards femtosecond on-chip electronics based on plasmonic hot electron nano-emitters," Nature Communications **9**, 1–7 (2018).

[22] Philipp Zimmermann, Alexander Hötger, Noelia Fernandez, Anna Nolinder, Kai Müller, Jonathan J. Finley, and Alexander W. Holleitner, "Toward Plasmonic Tunnel Gaps for Nanoscale Photoemission Currents by On-Chip Laser Ablation," Nano Letters **19**, 1172–1178 (2019).

[23] Shambhu Ghimire, Anthony D. DiChiara, Emily Sistrunk, Pierre Agostini, Louis F. DiMauro, and David A. Reis, "Observation of high-order harmonic generation in a bulk crystal," Nature Physics **7**, 138–141 (2010).

[24] Martin Schultze, Elisabeth M. Bothschafter, Annkatrin Sommer, Simon Holzner, Wolfgang Schweinberger, Markus Fiess, Michael Hofstetter, Reinhard Kienberger, Vadym Apalkov, Vladislav S. Yakovlev, Mark I. Stockman, and Ferenc Krausz, "Controlling dielectrics with the electric field of light," Nature **493**, 75–78 (2012).

[25] G. Vampa, T.J. Hammond, N. Thiré, B.E. Schmidt, F. Légaré, C.R. McDonald, T. Brabec, D.D. Klug, and P.B. Corkum, "All-optical reconstruction of crystal band structure," Physical Review Letters **115** (2015), 10.1103/physrevlett.115.193603.

[26] Agustin Schiffrin, Tim Paasch-Colberg, Nicholas Karpowicz, Vadym Apalkov, Daniel Gerster, Sascha Mühlbrandt, Michael Korbman, Joachim Reichert, Martin Schultze, Simon Holzner, Johannes V. Barth, Reinhard Kienberger, Ralph Ernstorfer, Vladislav S. Yakovlev, Mark I. Stockman, and Ferenc Krausz, "Optical-field-induced current in dielectrics," Nature **493**, 70–74 (2013).

[27] O. Schubert, M. Hohenleutner, F. Langer, B. Urbanek, C. Lange, U. Huttner, D. Golde, T. Meier, M. Kira, S. W. Koch, and R. Huber, "Sub-cycle control of terahertz high-harmonic generation by dynamical Bloch oscillations," Nature Photonics **8**, 119–123 (2014).

[28] Martin Schultze, Krupa Ramasesha, C.D. Pemmaraju, S.A. Sato, D. Whitmore, A. Gandman, James S. Prell, L. J. Borja, D. Prendergast, K. Yabana, Daniel M. Neumark, and Stephen R. Leone, "Attosecond band-gap dynamics in silicon," Science **346**, 1348–1352 (2014).

[29] M. Hohenleutner, F. Langer, O. Schubert, M. Knorr, U. Huttner, S. W. Koch, M. Kira, and R. Huber, "Real-time observation of interfering crystal electrons in high-harmonic generation," Nature **523**, 572–575 (2015).

[30] Takuya Higuchi, Christian Heide, Konrad Ullmann, Heiko B. Weber, and Peter Hommelhoff, "Light-field-driven currents in graphene," Nature **550**, 224–228 (2017).

[31] Shambhu Ghimire and David A. Reis, "High-harmonic generation from solids," Nature Physics **15**, 10–16 (2018).

[32] Tobias Boolakee, Christian Heide, Fabian Wagner, Christian Ott, Maria Schlecht, Jürgen Ristein, Heiko B Weber, and Peter Hommelhoff, "Length-dependence of light-induced cur-

rents in graphene," Journal of Physics B: Atomic, Molecular and Optical Physics **53**, 154001 (2020).

[33] Christian Heide, Tobias Boolakee, Takuya Higuchi, Heiko B. Weber, and Peter Hommelhoff, "Interaction of carrier envelope phase-stable laser pulses with graphene: The transition from the weak-field to the strong-field regime," New Journal of Physics **21** (2019), 10.1088/1367-2630/ab13ce.

[34] Christian Heide, Tobias Boolakee, Timo Eckstein, and Peter Hommelhoff, "Optical current generation in graphene: CEP control vs. $\omega + 2\omega$ control," Nanophotonics **10**, 3701–3707 (2021).

[35] Tobias Weitz, Christian Heide, and Peter Hommelhoff, "Strong-field bloch electron interferometry for band-structure retrieval," Physical Review Letters **132** (2024), 10.1103/physrevlett.132.206901.

[36] Fabian Langer, Yen-Po Liu, Zhe Ren, Vidar Flodgren, Chen Guo, Jan Vogelsang, Sara Mikaelsson, Ivan Sytcevich, Jan Ahrens, Anne L'Huillier, Cord L. Arnold, and Anders Mikkelsen, "Few-cycle lightwave-driven currents in a semiconductor at high repetition rate," Optica **7**, 276 (2020).

[37] Tim Paasch-Colberg, Stanislav Yu. Kruchinin, Özge Sağlam, Stefan Kapser, Stefano Cabrini, Sascha Muehlbrandt, Joachim Reichert, Johannes V. Barth, Ralph Ernstorfer, Reinhard Kienberger, Vladislav S. Yakovlev, Nicholas Karpowicz, and Agustin Schiffrin, "Sub-cycle optical control of current in a semiconductor: from the multiphoton to the tunneling regime," Optica **3**, 1358 (2016).

[38] Václav Hanus, Viktória Csajbók, Zsuzsanna Pápa, Judit Budai, Zsuzsanna Márton, Gellért Zsolt Kiss, Péter Sándor, Pallabi Paul, Adriana Szeghalmi, Zilong Wang, Boris Bergues, Matthias F. Kling, György Molnár, János Volk, and Péter Dombi, "Light-field-driven current control in dielectrics with pJ-Level laser pulses at 80 MHz repetition rate," Optica **8** (2021), 10.1364/optica.420360.

[39] Ojoon Kwon, Tim Paasch-Colberg, Vadym Apalkov, Bum-Kyu Kim, Ju-Jin Kim, Mark I. Stockman, and D. Kim, "Semimetallization of dielectrics in strong optical fields," Scientific Reports **6** (2016), 10.1038/srep21272.

[40] Ojoon Kwon and D. Kim, "PHz current switching in calcium fluoride single crystal," Applied Physics Letters **108** (2016), 10.1063/1.4949487.

[41] Ferenc Krausz and Mark I. Stockman, "Attosecond metrology: from electron capture to future signal processing," Nature Photonics **8**, 205–213 (2014).

[42] M. Garg, M. Zhan, T. T. Luu, H. Lakhotia, T. Klostermann, A. Guggenmos, and E. Goulielmakis, "Multi-petahertz electronic metrology," Nature **538**, 359–363 (2016).

[43] Tobias Boolakee, Christian Heide, Antonio Garzón-Ramírez, Heiko B. Weber, Ignacio Franco, and Peter Hommelhoff, "Light-field control of real and virtual charge carriers," Nature **605**, 251–255 (2022).

[44] Christian Heide, Takuya Higuchi, Heiko B. Weber, and Peter Hommelhoff, "Coherent Electron Trajectory Control in Graphene," Physical Review Letters **121**, 207401 (2018).

[45] J. D. Lee, Youngjae Kim, and Chil-Min Kim, "Model for petahertz optical memory based on a manipulation of the optical-field-induced current in dielectrics," New Journal of Physics **20**, 093029 (2018).

[46] F. Langer, C. P. Schmid, S. Schlauderer, M. Gmitra, J. Fabian, P. Nagler, C. Schüller, T. Korn, P. G. Hawkins, J. T. Steiner, U. Huttner, S. W. Koch, M. Kira, and R. Huber, "Lightwave valleytronics in a monolayer of tungsten diselenide," Nature **557**, 76–80 (2018).

[47] Sangeeta Sharma, Peter Elliott, and Samuel Shallcross, "Thz induced giant spin and valley currents," Science Advances **9** (2023), 10.1126/sciadv.adf3673.

[48] Sangeeta Sharma, Deepika Gill, and Samuel Shallcross, "Giant and controllable valley currents in graphene by double pumped thz light," Nano Letters **23**, 10305–10310 (2023).

[49] Sambit Mitra, Álvaro Jiménez-Galán, Mario Aulich, Marcel Neuhaus, Rui E. F. Silva, Volodymyr Pervak, Matthias F. Kling, and Shubhadeep Biswas, "Light-wave-controlled haldane model in monolayer hexagonal boron nitride," Nature **628**, 752–757 (2024).

[50] Igor Tyulnev, Álvaro Jiménez-Galán, Julita Poborska, Lenard Vamos, Philip St. J. Russell, Francesco Tani, Olga Smirnova, Misha Ivanov, Rui E. F. Silva, and Jens Biegert, "Valleytronics in bulk mos2 with a topologic optical field," Nature **628**, 746–751 (2024).

[51] Dandan Hui, Husain Alqattan, Simin Zhang, Vladimir Pervak, Enam Chowdhury, and Mohammed Th. Hassan, "Ultrafast optical switching and data encoding on synthesized light fields," Science Advances **9** (2023), 10.1126/sciadv.adf1015.

[52] Mohammed Th. Hassan, "Lightwave electronics: Attosecond optical switching," ACS Photonics (2024), 10.1021/acsphotonics.3c01584.

[53] Shawn Sederberg, Dmitry Zimin, Sabine Keiber, Florian Siegrist, Michael S. Wismer, Vladislav S. Yakovlev, Isabella Floss, Christoph Lemell, Joachim Burgdörfer, Martin Schultze, Ferenc Krausz, and Nicholas Karpowicz, "Attosecond optoelectronic field measurement in solids," Nature Communications **11**, 1–8 (2020).

[54] Yangyang Liu, Shima Gholam-Mirzaei, John E. Beetar, Jonathan Nesper, Ahmed Yousif, M. Nrisimhamurty, Michael Chini, and Michael Chini, "All-optical sampling of few-cycle infrared pulses using tunneling in a solid," Photonics Research **9**, 929–936 (2021).

[55] Johannes Blöchl, Johannes Schötz, Ancyline Maliakkal, Natālija Šreibere, Zilong Wang, Philipp Rosenberger, Peter Hommelhoff, Andre Staudte, Paul B. Corkum, Boris Bergues, and Matthias F. Kling, "Spatiotemporal sampling of near-petahertz vortex fields," Optica **9**, 755–761 (2022).

[56] Dmitry A. Zimin, Nicholas Karpowicz, Muhammad Qasim, Matthew Weidman, Ferenc Krausz, and Vladislav S. Yakovlev, "Dynamic optical response of solids following 1-fs-scale photoinjection," Nature **618** (2023), 10.1038/s41586-023-05986-w.

[57] Ya Bai, Fucong Fei, Shuo Wang, Na Li, Xiaolu Li, Fengqi Song, Ruxin Li, Zhizhan Xu, and Peng Liu, "High-harmonic generation from topological surface states," Nature Physics (2020), 10.1038/s41567-020-01052-8.

[58] Denitsa Baykusheva, Alexis Chacón, Jian Lu, Trevor P. Bailey, Jonathan A. Sobota, Hadas Soifer, Patrick S. Kirchmann, Costel Rotundu, Ctirad Uher, Tony F. Heinz, David A. Reis, and Shambhu Ghimire, "All-optical probe of three-dimensional topological insulators based on high-harmonic generation by circularly polarized laser fields," Nano Letters **21**, 8970–8978 (2021).

[59] C P Schmid, L Weigl, P Grössing, V Junk, C Gorini, S Schlauderer, S Ito, M Meierhofer, N Hofmann, D Afanasiev, J Crewse, K A Kokh, O E Tereshchenko, J Güdde, F Evers, J Wilhelm, K Richter, U Höfer, and R Huber, "generation in a topological insulator," Nature **593** (2021), 10.1038/s41586-021-03466-7.

[60] Christian Heide, Yuki Kobayashi, Denitsa R Baykusheva, Deepti Jain, Jonathan A Sobota, Patrick S Kirchmann, Tony F Heinz, David A Reis, and Shambhu Ghimire, "Probing topological phase transitions using high-harmonic generation," Nature Photonics **16**, 620–624 (2022).

[61] N. Tancogne-Dejean, M. A. Sentef, and A. Rubio, "Ultrafast modification of hubbard u in a strongly correlated material: *ab initio* high-harmonic generation in nio," Physical Review Letters **121**, 097402 (2018).

[62] Y. Kawakami, T. Amano, H. Ohashi, H. Itoh, Y. Nakamura, H. Kishida, T. Sasaki, G. Kawaguchi, H. M. Yamamoto, K. Yamamoto, S. Ishihara, K. Yonemitsu, and S. Iwai, "Petahertz non-linear current in a centrosymmetric organic superconductor," Nature Communications **11** (2020), 10.1038/s41467-020-17776-3.

[63] A. Pizzi, A. Gorlach, N. Rivera, A. Nunnenkamp, and I. Kaminer, "Light emission from strongly driven many-body systems," Nature Physics **19**, 551 (2023).

[64] Florian Siegrist, Julia A. Gessner, Marcus Ossiander, Christian Denker, Yi-Ping Chang, Malte C. Schröder, Alexander Guggenmos, Yang Cui, Jakob Walowski, Ulrike Martens, J. K. Dewhurst, Ulf Kleineberg, Markus Münzenberg, Sangeeta Sharma, and Martin Schultze, "Light-wave dynamic control of magnetism," Nature **571**, 240–244 (2019).

[65] Markus Borsch, Manuel Meierhofer, Rupert Huber, and Mackillo Kira, "Lightwave electronics in condensed matter," Nature Reviews Materials **8**, 668–687 (2023).

[66] Felix Bloch, "Über die quantenmechanik der elektronen in kristallgittern," Zeitschrift für Physik **52**, 555–600 (1929).

[67] L V Keldysh, "Ionization in the field of a strong electromagnetic wave," Soviet Physics JETP **20** (1964).

[68] Martin Wegener, Extreme Nonlinear Optics (Springer-Verlag, 2005).

[69] Christian Heide, Tobias Boolakee, Takuya Higuchi, and Peter Hommelhoff, "Adiabaticity parameters for the categorization of light-matter interaction: From weak to strong driving," Physical Review A **104** (2021), 10.1103/physreva.104.023103.

[70] Stanislav Yu. Kruchinin, Ferenc Krausz, and Vladislav S. Yakovlev, "icolloquium/i : Strong-field phenomena in periodic systems," Reviews of Modern Physics **90** (2018), 10.1103/revmodphys.90.021002.

[71] Th. Udem, R. Holzwarth, and T. W. Hänsch, "Optical frequency metrology," Nature **416**, 233–237 (2002).

[72] A. Wirth, M. Th Hassan, I. Grguraš, J. Gagnon, A. Moulet, T. T. Luu, S. Pabst, R. Santra, Z. A. Alahmed, A. M. Azzeer, V. S. Yakovlev, V. Pervak, F. Krausz, and E. Goulielmakis, "Synthesized light transients," Science **334**, 195–200 (2011).

[73] Björn Piglosiewicz, Slawa Schmidt, Doo Jae Park, Jan Vogelsang, Petra Groß, Cristian Manzoni, Paolo Farinello, Giulio Cerullo, and Christoph Lienau, "Carrier-envelope phase effects on the strong-field photoemission of electrons from metallic nanostructures," Nature Photonics **8**, 37–42 (2014).

[74] Johannes Schötz, Ancyline Maliakkal, Johannes Blöchl, Dmitry Zimin, Zilong Wang, Philipp Rosenberger, Meshaal Alharbi, Abdallah M. Azzeer, Matthew Weidman, Vladislav S. Yakovlev, Boris Bergues, and Matthias F. Kling, "The emergence of macroscopic currents in photoconductive sampling of optical fields," Nature Communications **13** (2022), 10.1038/s41467-022-28412-7.

[75] Markus Ludwig, Garikoitz Aguirregabiria, Felix Ritzkowsky, Tobias Rybka, Dana Codruta Marinica, Javier Aizpurua, Andrei G. Borisov, Alfred Leitenstorfer, and Daniele Brida, "Sub-femtosecond electron transport in a nanoscale gap," Nature Physics **16**, 341–345 (2020).

[76] Liping Shi, Ihar Babushkin, Anton Husakou, Oliver Melchert, Bettina Frank, Juemin Yi, Gustav Wetzel, Ayhan Demircan, Christoph Lienau, Harald Giessen, Misha Ivanov, Uwe Morgner, and Milutin Kovacev, "Femtosecond field-driven on-chip unidirectional electronic currents in nonadiabatic tunneling regime," Laser amp; Photonics Reviews **15** (2021), 10.1002/lpor.202000475.

[77] Gershon Kurizki, Moshe Shapiro, and Paul Brumer, "Phase-coherent control of photocurrent directionality in semiconductors," Physical Review B **39**, 3435–3437 (1989).

[78] A. Haché, Y. Kostoulas, R. Atanasov, J. L.P. Hughes, J. E. Sipe, and Max Glasbeek, "Observation of coherently controlled photocurrent in unbiased, bulk GaAs," Physical Review Letters **78**, 306–309 (1997).

[79] T. M. Fortier, P. A. Roos, D. J. Jones, S. T. Cundiff, R. D.R. Bhat, and J. E. Sipe, "Carrier-envelope phase-controlled quantum interference of injected photocurrents in semiconductors," Physical Review Letters **92**, 1–4 (2004).

[80] Dong Sun, Charles Divin, Julien Rioux, John E. Sipe, Claire Berger, Walt A. De Heer, Phillip N. First, and Theodore B. Norris, "Coherent control of ballistic photocurrents in multilayer epitaxial graphene using quantum interference," Nano Letters **10**, 1293–1296 (2010).

[81] Lev Landau, "Zur theorie der energieubertragung. ii," Physikalische Zeitschrift der Sowjetunion **2**, 46 (1932).

[82] Clarence Zener, "A theory of the electrical breakdown of solid dielectrics," Proceedings of the Royal Society of London. Series A, Containing Papers of a Mathematical and Physical Character **145**, 523–529 (1934).

[83] ECG Stueckelberg, "Theorie der unelastischen stösse zwischen atomen," Helv. Phys. Acta **5**, 369 (1932).

[84] Ettore Majorana, "Atomi orientati in campo magnetico variabile," Il Nuovo Cimento (1924-1942) **9**, 43–50 (1932).

[85] Christian Heide, Tobias Boolakee, Takuya Higuchi, and Peter Hommelhoff, "Sub-cycle temporal evolution of light-induced electron dynamics in hexagonal 2d materials," Journal of Physics: Photonics **2**, 024004 (2020).

[86] Kenichi L. Ishikawa, "Nonlinear optical response of graphene in time domain," Physical Review B **82** (2010), 10.1103/physrevb.82.201402.

[87] Kenichi L Ishikawa, "Electronic response of graphene to an ultrashort intense terahertz radiation pulse," New Journal of Physics **15**, 055021 (2013).

[88] Hamed Koochaki Kelardeh, Vadym Apalkov, and Mark I. Stockman, "Graphene in ultrafast and superstrong laser fields," Physical Review B **91** (2015), 10.1103/physrevb.91.045439.

[89] Tong Wu, Guanglu Yuan, Zishao Wang, Xiangyu Zhang, Chao Yu, and Ruifeng Lu, "Carrier-envelope phase-controlled residual current in semiconductors," Symmetry **15**, 784 (2023).

[90] Q. Z. Li, P. Elliott, J. K. Dewhurst, S. Sharma, and S. Shallcross, "Ab initio study of ultrafast charge dynamics in graphene," Physical Review B **103** (2021), 10.1103/physrevb.103.l081102.

[91] Ofer Neufeld, Nicolas Tancogne-Dejean, Umberto De Giovannini, Hannes Hübener, and Angel Rubio, "Light-driven extremely nonlinear bulk photogalvanic currents," Physical Review Letters **127** (2021), 10.1103/physrevlett.127.126601.

[92] Yuya Morimoto, Yasushi Shinohara, Kenichi L Ishikawa, and Peter Hommelhoff, "Atomic real-space perspective of light-field-driven currents in graphene," New Journal of Physics **24**, 033051 (2022).

[93] Liping Chen, Yu Zhang, Guanhua Chen, and Ignacio Franco, "Stark control of electrons along nanojunctions," Nature Communications **9**, 1–12 (2018).

[94] Christian Heide, Timo Eckstein, Tobias Boolakee, Constanze Gerner, Heiko B. Weber, Ignacio Franco, and Peter Hommelhoff, "Electronic coherence and coherent dephasing in the optical control of electrons in graphene," Nano Letters **21**, 9403–9409 (2021).

[95] S. Azar Oliaei Motlagh, Jhih-Sheng Wu, Vadym Apalkov, and Mark I. Stockman, "Fundamentally fastest optical processes at the surface of a topological insulator," Physical Review B **98** (2018), 10.1103/physrevb.98.125410.

[96] Amar Bharti and Gopal Dixit, "Tailoring photocurrent in weyl semimetals via intense laser irradiation," Physical Review B **108** (2023), 10.1103/physrevb.108.l161113.

[97] Jiayin Chen, Candong Liu, Zhinan Zeng, and Ruxin Li, "Control of ultrafast photocurrent in twisted bilayer graphene by circularly polarized few-cycle lasers," Physical Review B **105** (2022), 10.1103/physrevb.105.014309.

[98] Pardeep Kumar, Thakshila M Herath, and Vadym Apalkov, "Bilayer graphene in strong ultrafast laser fields," Journal of Physics: Condensed Matter **33**, 335305 (2021).

[99] Erheng Wu, Chaojin Zhang, Zhanshan Wang, and Chengpu Liu, "Waveform control of currents in graphene by chirped few-cycle lasers," New Journal of Physics **22**, 033016 (2020).

[100] Dandan Hui, Husain Alqattan, Shunsuke Yamada, Vladimir Pervak, Kazuhiro Yabana, and Mohammed Th Hassan, "Attosecond electron motion control in dielectric," Nature Photonics **16**, 33–37 (2022).

[101] Xiaoxue Zhang, Henglei Du, Wenkang Wang, Huicheng Guo, and Chengpu Liu, "Residual current under the combined effect of carrier envelope phase and chirp: phase shift and peak enhancement," Optics Express **31**, 26879 (2023).

[102] Xiaoxue Zhang, Erheng Wu, Henglei Du, Huicheng Guo, and Chengpu Liu, "Bidirectional residual current in monolayer graphene under few-cycle laser irradiation," Optics Express **30**, 37863 (2022).

[103] Á. Jiménez-Galán, R. E. F. Silva, O. Smirnova, and M. Ivanov, "Lightwave control of topological properties in 2d materials for sub-cycle and non-resonant valley manipulation," Nature Photonics **14**, 728–732 (2020).

[104] S. Azar Oliaei Motlagh and Vadym Apalkov, "Anomalous ultrafast all-optical hall effect in gapped graphene," Nanophotonics **10**, 3677–3685 (2021).

[105] Arqum Hashmi, Shunsuke Yamada, Atsushi Yamada, Kazuhiro Yabana, and Tomohito Otobe, "Valley polarization control in ¡mml:math xmlns:mml="http://www.w3.org/1998/math/mathml"¿¡mml:msub¿¡mml:mi¿wse¡/mml:mi¿¡mml:mn¿2¡/mn monolayer by a single-cycle laser pulse," Physical Review B **105** (2022), 10.1103/physrevb.105.115403.

[106] Shawn Sederberg, Fanqi Kong, Felix Hufnagel, Chunmei Zhang, Ebrahim Karimi, and Paul B. Corkum, "Vectorized optoelectronic control and metrology in a semiconductor," Nature Photonics **14**, 680–685 (2020).

[107] Shawn Sederberg and Paul B. Corkum, "Perspective on phase-controlled currents in semiconductors driven by structured light," Applied Physics Letters **120** (2022), 10.1063/5.0089345.

[108] K. Jana, K. R. Herperger, F. Kong, Y. Mi, C. Zhang, P. B. Corkum, and S. Sederberg, "Reconfigurable electronic circuits for magnetic fields controlled by structured light," Nature Photonics **15**, 622–626 (2021).

[109] Jacob Pettine, Prashant Padmanabhan, Teng Shi, Lauren Gingras, Luke McClintock, Chun-Chieh Chang, Kevin W. C. Kwock, Long Yuan, Yue Huang, John Nogan, Jon K. Baldwin, Peter Adel, Ronald Holzwarth, Abul K. Azad, Filip Ronning, Antoinette J. Taylor, Rohit P. Prasankumar, Shi-Zeng Lin, and Hou-Tong Chen, "Light-driven nanoscale vectorial currents," Nature (2024), 10.1038/s41586-024-07037-4.

[110] M. S. Mrudul, Álvaro Jiménez-Galán, Misha Ivanov, and Gopal Dixit, "Light-induced valleytronics in pristine graphene," Optica **8**, 422 (2021).

[111] M. Ossiander, K. Golyari, K. Scharl, L. Lehnert, F. Siegrist, J. P. Bürger, D. Zimin, J. A. Gessner, M. Weidman, I. Floss, V. Smejkal, S. Donsa, C. Lemell, F. Libisch, N. Karpowicz, J. Burgdörfer, F. Krausz, and M. Schultze, "The speed limit of optoelectronics," Nature Communications **13**, 1–8 (2022).

[112] Antonio J. Garzón-Ramírez and Ignacio Franco, "Stark control of electrons across interfaces," Physical Review B **98** (2018), 10.1103/physrevb.98.121305.

[113] Aldo Di Carlo, P. Vogl, and W. Pötz, "Theory of zener tunneling and wannier-stark states in semiconductors," Physical Review B **50**, 8358–8377 (1994).

[114] Maxim Durach, Anastasia Rusina, Matthias F. Kling, and Mark I. Stockman, "Metallization of nanofilms in strong adiabatic electric fields," Physical Review Letters **105** (2010), 10.1103/physrevlett.105.086803.

[115] Georg Wachter, Christoph Lemell, Joachim Burgdörfer, Shunsuke A. Sato, Xiao-Min Tong, and Kazuhiro Yabana, "iab initio/isimulation of electrical currents induced by ultrafast laser excitation of dielectric materials," Physical Review Letters **113** (2014), 10.1103/physrevlett.113.087401.

[116] Ignacio Franco, Moshe Shapiro, and Paul Brumer, "Robust ultrafast currents in molecular wires through stark shifts," Physical Review Letters **99** (2007), 10.1103/physrevlett.99.126802.

[117] Antonio J. Garzón-Ramírez and Ignacio Franco, "Symmetry breaking in the Stark Control of Electrons at Interfaces (SCELI)," Journal of Chemical Physics **153** (2020), 10.1063/5.0013190.

[118] Antonio J. Garzón-Ramírez, Francisco Fernández Villoria, and Ignacio Franco, "Screening and band bending effects in the stark control of electrons at interfaces (SCELI)," Physical Review B **103** (2021), 10.1103/physrevb.103.235304.

[119] S. Yu. Kruchinin, M. Korbman, and V. S. Yakovlev, "Theory of strong-field injection and control of photocurrent in dielectrics and wide band gap semiconductors," Physical Review B **87** (2013), 10.1103/physrevb.87.115201.

[120] Jacob B. Khurgin, "Optically induced currents in dielectrics and semiconductors as a nonlinear optical effect," Journal of the Optical Society of America B **33**, C1 (2015).

[121] Antonio J. Garzón-Ramírez and Ignacio Franco, "Symmetry breaking in the stark control of electrons at interfaces (sceli)," The Journal of Chemical Physics **153** (2020), 10.1063/5.0013190.

[122] Antonio J. Garzón-Ramírez and Ignacio Franco, "Stark control of electrons across interfaces," Physical Review B **98** (2018), 10.1103/physrevb.98.121305.

[123] Peter Hommelhoff, Yvan Sortais, Anoush Aghajani-Talesh, and Mark A. Kasevich, "Field emission tip as a nanometer source of free electron femtosecond pulses," Physical Review Letters **96** (2006), 10.1103/physrevlett.96.077401.

[124] Peter Hommelhoff, Catherine Kealhofer, and Mark A. Kasevich, "Ultrafast electron pulses from a tungsten tip triggered by low-power femtosecond laser pulses," Physical Review Letters **97** (2006), 10.1103/physrevlett.97.247402.

[125] C. Ropers, D. R. Solli, C. P. Schulz, C. Lienau, and T. Elsaesser, "Localized multiphoton emission of femtosecond electron pulses from metal nanotips," Physical Review Letters **98** (2007), 10.1103/physrevlett.98.043907.

[126] Michael Kruger, Markus Schenk, and Peter Hommelhoff, "Attosecond control of electrons emitted from a nanoscale metal tip," Nature **475**, 78–81 (2011).

[127] Björn Piglosiewicz, Slawa Schmidt, Doo Jae Park, Jan Vogelsang, Petra Groß, Cristian Manzoni, Paolo Farinello, Giulio Cerullo, and Christoph Lienau, "Carrier-envelope phase effects on the strong-field photoemission of electrons from metallic nanostructures," Nature Photonics **8**, 37–42 (2013).

[128] Adina R. Bechhofer, Shruti Nirantar, Luca Daniel, Karl K. Berggren, and Phillip D. Keathley, "Circuit model for nanoscale optical frequency electronics," in 2023 IEEE 36th International Vacuum Nanoelectronics Conference (IVNC) (IEEE, 2023).

[129] Michael E. Swanwick, Phillip D. Keathley, Arya Fallahi, Peter R. Krogen, Guillaume Laurent, Jeffrey Moses, Franz X. Kärtner, and Luis F. Velásquez-García, "Nanostructured Ultrafast Silicon-Tip Optical Field-Emitter Arrays," Nano Letters **14**, 5035–5043 (2014).

[130] Richard G. Hobbs, Yujia Yang, Arya Fallahi, Philip D. Keathley, Eva De Leo, Franz X. Kärtner, William S. Graves, and Karl K. Berggren, "High-Yield, Ultrafast, Surface Plasmon-Enhanced, Au Nanorod Optical Field Electron Emitter Arrays," ACS Nano **8**, 11474–11482 (2014).

[131] R. K. Li, H. To, G. Andonian, J. Feng, A. Polyakov, C. M. Scoby, K. Thompson, W. Wan, H. A. Padmore, and P. Musumeci, "Surface-Plasmon Resonance-Enhanced Multiphoton Emission of High-Brightness Electron Beams from a Nanostructured Copper Cathode," Physical Review Letters **110**, 074801 (2013).

[132] Philip Dienstbier, Lennart Seiffert, Timo Paschen, Andreas Liehl, Alfred Leitenstorfer, Thomas Fennel, and Peter Hommelhoff, "Tracing attosecond electron emission from a nanometric metal tip," Nature **616**, 702–706 (2023).

[133] H. Y. Kim, M. Garg, S. Mandal, L. Seiffert, T. Fennel, and E. Goulielmakis, "Attosecond field emission," Nature **613**, 662–666 (2023).

[134] M. Sivis, M. Duwe, B. Abel, and C. Ropers, "Extreme-ultraviolet light generation in plasmonic nanostructures," Nature Physics **9**, 304–309 (2013).

[135] Chi Li, Ke Chen, Mengxue Guan, Xiaowei Wang, Xu Zhou, Feng Zhai, Jiayu Dai, Zhenjun Li, Zhipei Sun, Sheng Meng, Kaihui Liu, and Qing Dai, "Extreme nonlinear strong-field photoemission from carbon nanotubes," Nature Communications **10**, 4891 (2019).

[136] Marco Turchetti, Yujia Yang, Mina Bionta, Alberto Nardi, Luca Daniel, Karl K. Berggren, and Phillip D. Keathley, "Electron Emission Regimes of Planar Nano Vacuum Emitters," IEEE Transactions on Electron Devices **69**, 3953–3959 (2022).

[137] Y. Mairesse and F. Qur, "Frequency-resolved optical gating for complete reconstruction of attosecond bursts," Physical Review A **71**, 011401 (2005).

[138] A. Herbst, K. Scheffter, M. M. Bidhendi, M. Kieker, A. Srivastava, and H. Fattahi, "Recent advances in petahertz electric field sampling," Journal of Physics B: Atomic, Molecular and Optical Physics **55** (2022), 10.1088/1361-6455/ac8032.

[139] A. Apolonski, P. Dombi, G. G. Paulus, M. Kakehata, R. Holzwarth, Th. Udem, Ch. Lemell, K. Torizuka, J. Burgdörfer, T. W. Hänsch, and F. Krausz, "Observation of Light-Phase-Sensitive Photoemission from a Metal," Physical Review Letters **92**, 073902 (2004).

[140] Felix Ritzkowsky, Matthew Yeung, Engjell Bebeti, Thomas Gebert, Toru Matsuyama, Matthias Budden, Roland Mainz, Huseyin Cankaya, Karl Berggren, Giulio Rossi, Phillip Keathley, and Franz Kärtner, "Large Area Optical Frequency Detectors for Single-Shot Phase Readout," (2023), arxiv:2306.01621 [physics].

[141] Dario Cattozzo Mor, Yujia Yang, Felix Ritzkowsky, Franz Kartner, Karl Berggren, Neetesh Singh, and Phillip Keathley, "PHz Electronic Device Design and Simulation for Waveguide-Integrated Carrier-Envelope Phase Detection," Journal of Lightwave Technology , 1–1 (2022).

[142] Dominik Hoff, Michael Krüger, Lothar Maisenbacher, A. M. Sayler, Gerhard G. Paulus, and Peter Hommelhoff, "Tracing the phase of focused broadband laser pulses," Nature Physics **13**, 947–951 (2017).

[143] Václav Hanus, Beatrix Fehér, Viktória Csajbók, Péter Sándor, Zsuzsanna Pápa, Judit Budai, Zilong Wang, Pallabi Paul, Adriana Szeghalmi, and Péter Dombi, "Carrier-envelope phase on-chip scanner and control of laser beams," Nature Communications **14** (2023), 10.1038/s41467-023-40802-z.

[144] Andrea Rossetti, Matthias Falk, Alfred Leitenstorfer, Daniele Brida, and Markus Ludwig, "Gouy phase effects on photocurrents in plasmonic nanogaps driven by single-cycle pulses," Nanophotonics **0** (2024), 10.1515/nanoph-2023-0897.

[145] Kai-Fu Wong, Weiwei Li, Zilong Wang, Vincent Wanie, Erik Månsson, Dominik Hoeing, Johannes Blöchl, Thomas Nubbemeyer, Abdallah Azzeer, Andrea Trabattoni, Holger Lange, Francesca Calegari, and Matthias F. Kling, "Far-field petahertz sampling of plasmonic fields," Nano Letters **24**, 5506–5512 (2024).

[146] J. Itatani, F. Quéré, G. L. Yudin, M. Yu. Ivanov, F. Krausz, and P. B. Corkum, "Attosecond Streak Camera," Physical Review Letters **88**, 173903 (2002).

[147] Seung Beom Park, Kyungseung Kim, Wosik Cho, Sung In Hwang, Igor Ivanov, Chang Hee Nam, and Kyung Taec Kim, "Direct sampling of a light wave in air," Optica **5**, 402–408 (2018).

[148] Wosik Cho, Sung In Hwang, Chang Hee Nam, Mina R. Bionta, Philippe Lassonde, Bruno E. Schmidt, Heide Ibrahim, François Légaré, and Kyung Taec Kim, "Temporal characterization of femtosecond laser pulses using tunneling ionization in the UV, visible, and mid-IR ranges," Scientific Reports **9**, 1–11 (2019).

[149] Yang Luo, Frank Neubrech, Alberto Martin-Jimenez, Na Liu, Klaus Kern, and Manish Garg, "Real-time tracking of coherent oscillations of electrons in a nanodevice by photo-assisted tunnelling," Nature Communications **15** (2024), 10.1038/s41467-024-45564-w.

[150] Dmitry A. Zimin, Vladislav S. Yakovlev, and Nicholas Karpowicz, "Ultra-broadband all-optical sampling of optical waveforms," Science Advances **8**, 1–7 (2022).

[151] Najd Altwaijry, Muhammad Qasim, Mikhail Mamaikin, Johannes Schötz, Keyhan Golyari, Michael Heynck, Enrico Ridente, Vladislav S. Yakovlev, Nicholas Karpowicz, and Matthias F. Kling, "Broadband Photoconductive Sampling in Gallium Phosphide," Advanced Optical Materials **11** (2023), 10.1002/adom.202202994.

[152] Yangyang Liu, John E. Beetar, Jonathan Nesper, Shima Gholam-Mirzaei, and Michael Chini, "Single-shot measurement of few-cycle optical waveforms on a chip," Nature Photonics **16**, 109–112 (2022).

[153] Abijith S. Kowligy, Henry Timmers, Alexander J. Lind, Ugaitz Elu, Flavio C. Cruz, Peter G. Schunemann, Jens Biegert, and Scott A. Diddams, "Infrared electric field sampled frequency comb spectroscopy," Science Advances **5** (2019), 10.1126/sciadv.aaw8794.

[154] Alexander Weigel, Philip Jacob, Wolfgang Schweinberger, Marinus Huber, Michael Trubetskov, Patrik Karandušovský, Christina Hofer, Theresa Buberl, Tatiana Amotchkina, Maximilian Högner, Daniel Hahner, Philipp Sulzer, Alfred Leitenstorfer, Vladimir Pervak, Ferenc Krausz, and Ioachim Pupeza, "Dual-oscillator infrared electro-optic sampling with attosecond precision," Optica **11**, 726 (2024).

[155] Ioachim Pupeza, Marinus Huber, Michael Trubetskov, Wolfgang Schweinberger, Syed A. Hussain, Christina Hofer, Kilian Fritsch, Markus Poetzlberger, Lenard Vamos, Ernst Fill, Tatiana Amotchkina, Kosmas V. Kepesidis, Alexander Apolonski, Nicholas Karpowicz, Vladimir Pervak, Oleg Pronin, Frank Fleischmann, Abdallah Azzeer, Mihaela Žigman, and Ferenc Krausz,

"Field-resolved infrared spectroscopy of biological systems," Nature **577**, 52–59 (2020).

[156] J. D. Lee, Won Seok Yun, and Noejung Park, "Rectifying the optical-field-induced current in dielectrics: Petahertz diode," Physical Review Letters **116** (2016), 10.1103/physrevlett.116.057401.

[157] Dario Cattozzo Mor, Yujia Yang, Felix Ritzkowsky, Franz X. Kartner, Karl K. Berggren, Neetesh Kumar Singh, and Phillip D. Keathley, "Phz electronic device design and simulation for waveguide-integrated carrier-envelope phase detection," Journal of Lightwave Technology **40**, 3823–3831 (2022).

[158] Ugaitz Elu, Luke Maidment, Lenard Vamos, Francesco Tani, David Novoa, Michael H. Frosz, Valeriy Badikov, Dmitrii Badikov, Valentin Petrov, Philip St. J. Russell, and Jens Biegert, "Seven-octave high-brightness and carrier-envelope-phase-stable light source," Nature Photonics **15**, 277–280 (2020).

[159] Philipp Steinleitner, Nathalie Nagl, Maciej Kowalczyk, Jinwei Zhang, Vladimir Pervak, Christina Hofer, Arkadiusz Hudzikowski, Jarosław Sotor, Alexander Weigel, Ferenc Krausz, and Ka Fai Mak, "Single-cycle infrared waveform control," Nature Photonics **16**, 512–518 (2022).

[160] Ferenc Krausz and Misha Ivanov, "Attosecond physics," Reviews of Modern Physics **81**, 163–234 (2009).

[161] Shu-Wei Huang, Giovanni Cirmi, Jeffrey Moses, Kyung-Han Hong, Siddharth Bhardwaj, Jonathan R. Birge, Li-Jin Chen, Enbang Li, Benjamin J. Eggleton, Giulio Cerullo, and Franz X. Kartner, "High-energy pulse synthesis with sub-cycle waveform control for strong-field physics," Nat Photon **5**, 475–479 (2011).

[162] David R. Carlson, Phillips Hutchison, Daniel D. Hickstein, and Scott B. Papp, "Generating few-cycle pulses with integrated nonlinear photonics," Optics Express **27**, 37374 (2019).

[163] Qiushi Guo, Benjamin K. Gutierrez, Ryoto Sekine, Robert M. Gray, James A. Williams, Luis Ledezma, Luis Costa, Arkadev Roy, Selina Zhou, Mingchen Liu, and Alireza Marandi, "Ultrafast mode-locked laser in nanophotonic lithium niobate," Science **382**, 708–713 (2023).

[164] Alexander Klenner, Aline S. Mayer, Adrea R. Johnson, Kevin Luke, Michael R. E. Lamont, Yoshitomo Okawachi, Michal Lipson, Alexander L. Gaeta, and Ursula Keller, "Gigahertz frequency comb offset stabilization based on supercontinuum generation in silicon nitride waveguides," Optics Express **24**, 11043 (2016).

[165] Tyler W. Hughes, Si Tan, Zhexin Zhao, Neil V. Sapra, Kenneth J. Leedle, Huiyang Deng, Yu Miao, Dylan S. Black, Olav Solgaard, James S. Harris, Jelena Vuckovic, Robert L. Byer, Shanhui Fan, R. Joel England, Yun Jo Lee, and Minghao Qi, "On-chip laser-power delivery system for dielectric laser accelerators," Physical Review Applied **9** (2018), 10.1103/physrevapplied.9.054017.

[166] Yoshitomo Okawachi, Mengjie Yu, Jaime Cardenas, Xingchen Ji, Alexander Klenner, Michal Lipson, and Alexander L. Gaeta, "Carrier envelope offset detection via simultaneous supercontinuum and second-harmonic generation in a silicon nitride waveguide," Optics Letters **43**, 4627 (2018).

[167] A. I. Ryzhov, O. V. Ivakhnenko, S. N. Shevchenko, M. F. Gonzalez-Zalba, and Franco Nori, "Alternative fast quantum logic gates using nonadiabatic landau-zener-stückelberg-majorana transitions," (2023).

[168] Joan J. Caceres, Daniel Dominguez, and Maria Jose Sanchez, "Fast quantum gates based on Landau-Zener-Stückelberg-Majorana transitions," (2023).

[169] Oleh V. Ivakhnenko, Sergey N. Shevchenko, and Franco Nori, "Nonadiabatic landau–zener–stückelberg–majorana transitions, dynamics, and interference," Physics Reports **995**, 1–89 (2023).

[170] Yee-Chia Yeo, Tsu-Jae King, and Chenming Hu, "Metal-dielectric band alignment and its implications for metal gate complementary metal-oxide-semiconductor technology," Journal of Applied Physics **92**, 7266–7271 (2002).

[171] Beatrix Fehér, Václav Hanus, Zsuzsanna Pápa, Judit Budai, Pallabi Paul, Adriana Szeghalmi, and Péter Dombi, "Laser-induced ultrafast currents in dielectrics enhanced by iridium nanoparticles," in Optica High-brightness Sources and Light-driven Interactions Congress 2022, HILAS (Optica Publishing Group, 2022).

[172] Najd Altwaijry, Muhammad Qasim, Dmitry Zimin, Nicholas Karpowicz, and Matthias F. Kling, "Sensitivity enhancement in photoconductive light field sampling," Advanced Optical Materials (2024), 10.1002/adom.202302490.

[173] Christian Heide, Martin Hauck, Takuya Higuchi, Jürgen Ristein, Lothar Ley, Heiko B. Weber, and Peter Hommelhoff, "Attosecond-fast internal photoemission," Nature Photonics **14**, 219–222 (2020).